DETERMINING FIXATION STABILITY OF AMD PATIENTS USING PREDICTIVE EYE ESTIMATION REGRESSION

A Thesis
Presented to
The Academic Faculty

by

Temilade A. Adelore

In Partial Fulfillment
of the Requirements for the Degree
Master of Science in the
School of Engineering

Georgia Institute of Technology
December 2008

DETERMINING FIXATION STABILITY OF AMD PATIENTS

USING PREDICTIVE EYE ESTIMATION REGRESSION

Approved by:

Eric Schumacher, Ph.D., Advisor
School of Psychology,
Georgia Institute of Technology

Stephen LaConte, Ph.D.
Department of Neuroscience
Baylor College of Medicine

Department of Biomedical Engineering
Rice University

Dr. Shella Kheilholz
Department of Biomedical Engineering
Georgia Institute of Technology

Date Approved: 07/18/08

ACKNOWLEDGEMENTS

I use this opportunity to thank my advisor Eric Schumacher for his encouragement, guidance and support. I also would like to thank Stephen LaConte, for without his foundational work on PEER, this thesis would not exist. Thank you for your willingness to collaborate, guide and support me throughout this project. I would like to thank the Emory Eye Clinic for their assistance in patient recruiting as well as the patients themselves for willingly participating in this project. Special thanks to Erin Kinzel and Keith Main for their time and technical contributions to this project. I will also like to thank my fellow members of CoNTRoL (Cognitive Neuroscience at Tech Research Laboratory) for the useful questions and comments. Finally, I sincerely thank my family and friends for their support and constant encouragement through out my time so far in graduate school.

TABLE OF CONTENTS

LIST OF TABLES

LIST OF FIGURES

SUMMARY

The Preferred Retinal Locus (PRL) is a preserved area of the peripheral retina that many AMD patients adopt as a fixation reference to replace the fovea. This new point of fixation is necessitated from the development of a central scotoma that arises in macular degeneration. Eye movements made while fixating with the PRL have been observed to be mal-adaptive compared to those made while fixating with the fovea. For example eye movements while fixating with the PRL negatively affect fixation stability and fixation precision; consequently creating difficulty in reading and limits to an AMD patient's execution of other everyday activities.

Abnormal eye movements as a result of the PRL also affect research investigations into physiological adaptations associated with AMD. Previous research investigating cortical reorganization in AMD patients from our group exposed the need to accurately determine an AMD patient's point of gaze in order to better infer cortical reorganization from consistent and regular use of a PRL. However the poor fixation performance experienced by AMD patients makes this task difficult to achieve.

In light of these issues, this research attempted to control fixation instability in AMD patients by determining point of gaze during fixation in a functional magnetic resonance imaging (fMRI) environment. The research method used is an MRI based technique called Predictive Eye Estimation Regression (PEER). PEER is an alternative and more favorable approach to the eye tracker in the MRI environment. It works by using eye positions (via voxel intensities in the scanned image) made during calibration runs to estimate a trained model to accurately predict subsequent points of gaze.

Abnormal eye movements in patients with AMD increase data complexity and negatively affect PEER's ability to estimate eye position. To resolve this issue, techniques to reduce eye movement abnormality effects were explored and implemented. Fixation stability was enhanced by ensuring optimal contrast through the use of a flashing stimulus target in all visual tasks. Each

participant's visual field was mapped in terms of retinal sensitivity to determine visual acuity and hence the appropriate size of the presented stimulus.

In adapting PEER for use with AMD patients, parameters such as temporal resolution and brain coverage were used to obtain optimal estimations of eye position. Also all participants were evaluated on different fixation protocols and the results compared to that of the micro-perimeter MP-1 to test the efficacy of PEER.

The fixation stability results obtained from PEER were similar to that obtained from the eye tracking results of the micro-perimeter MP-1. However, PEER's point of gaze estimations was different from the MP-1's in both the four cross and single cross fixation tests. The difference in this result cannot be concluded to be specific to PEER. In order to resolve this issue, advancements to PEER by the inclusion of an eye tracker in the scanner to run concurrently with PEER could provide more evidence of PEER's reliability. In addition, increasing the diversity of AMD patients in terms of the different scotoma types will help provide a better estimate of PEER flexibility and robustness.

CHAPTER 1: MACULAR DEGENERATION

Age-related Macular Degeneration (AMD) is medical condition that afflicts one in ten people over 80 in the United States (Cheung and Legge, 2005). According to the American Academy of Ophthalmology, it is also the leading cause of blindness in the U.S. for those over fifty. As of 2000, a total of 1.75 million Americans were diagnosed with AMD and this number is projected to rise to nearly 3million by 2020. Macular degeneration can also appear in younger individuals. In this case the disease is called Juvenile macular degeneration disease and results from a genetic variant. Both AMD and JMD affect the fovea and macula – the central 10 – 15 degrees of the visual field (Feret et. al, 2007) and have the potential to substantially reduce quality of life. For example, the progression of MD results in difficulty reading, difficulty driving, increased reliance on bright light and blurred or distorted vision.

1.1 Physiology of MD

There are two types of AMD: dry and wet. Dry AMD is often characterized by geographic atrophy confined to areas of cell death in the retinal pigment epithelium (RPE) layer. This type of AMD eventually causes dysfunction of the overlying photoreceptors leading to vision loss (Cheung and Legge, 2005). Wet, or neovascular, AMD, on the other hand, causes vision loss due to abnormal blood vessel growth in the chorio-capillaries. These aberrant vessels often break causing blood and protein leakage below the macula, eventually causing irreversible damage to the photoreceptors and if left untreated rapid vision loss.

1.2 Scotomata

Scotoma is an area of impaired visual acuity surrounded by relatively well-preserved peripheral vision. The formation of scotoma is a direct consequence of the retinal damage caused by either wet or dry AMD. At the onset of MD, the scotoma usually has a diameter of 10 degrees or

less, however at the advanced stage its diameter can range between 10 to 20 degrees (Cheung and Legge, 2005).

Scotomata appear in a variety of forms in the visual field. There are central, peripheral and bilateral scotomata (with the bilateral case occurring in both eyes at the same region of the visual field). The central or bilateral central scotoma is the form frequently found in MD patients. Scotomata also been found that central scotomata come in a variety of shapes, for example there are circular or ring-shaped scotoma surrounding a functional fovea (Cheung and Legge, 2005).

I 

II 

Figure 1: Normal Vision (I) Scotoma Obstructing Central Vision (II)

I: Normal vision courtesy of NIH National Eye Institute

II: Same view with age-related macular degeneration

The form, extent or the number of scotomata present in MD patients can be determined during standard assessments of the visual field (macular perimetry). Previous research has shown that the scotoma, depending on its form and shape, affects the level of fixation stability and visual acuity a patient experiences. Specifically, patients with ring shaped scotoma were found to have better fixation stability than those with central scotoma. In addition, visual acuity in patients with dense central scotoma was found to be significantly worse than in patients with dense ring scotoma (Mori et. al, 2001).

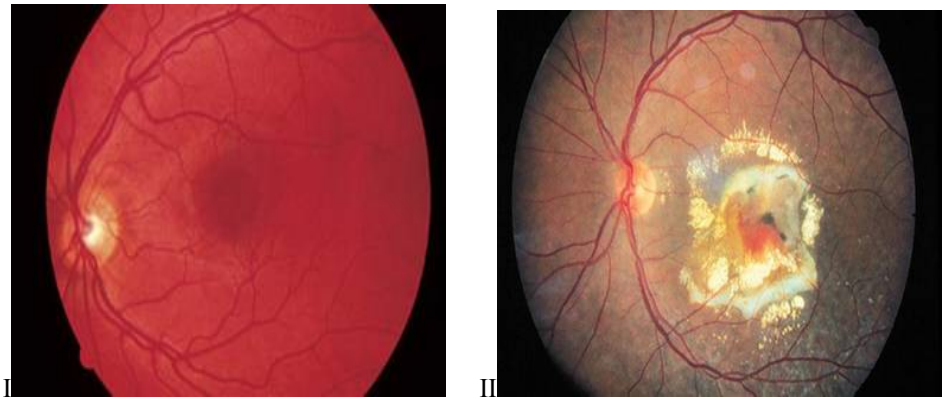

Figure 2: Healthy Retina (I) and Retina with MD (II)

I: The fovea is clearly visible

II: A dense central scotoma is present with a total loss of photoreceptors at the fovea

1.3 Preferred Retinal Locations

When MD patients are asked to attend to a visual target, they typically use an area in the peripheral retina instead of the fovea as a means to view the target. This new fixation reference is called a preferred retinal locus (PRL). MD patients adopt this new area for fixation because of the poor visual acuity at the fovea (Pidcoe and Wetzel, 2006). The PRL thus provides MD patients with the necessary strategy to continue performing everyday tasks. This method of viewing objects with the PRL is referred to as eccentric fixation.

PRL formation is a dynamic process. It depends on a variety of factors such as time since disease onset and the extent to which the scotoma obstructs the visual field. In the latter case, a large absolute scotoma might necessitate a PRL, while smaller horseshoe shaped scotomata might not because the fovea is still intact. PRL formation is also facilitated by other preserved peripheral areas becoming non-functional. Sometimes more than one PRL forms causing patients to use different PRLs for different tasks or at different luminance levels (Lei & Schuchard, 1997). No research has described a consistent pattern for how new PRLs develop. For instance Fletcher and Schuchard (1999) reported macular scotoma in 99 subjects to be 22% to the right, 15% to the left, 26% to both

the right and left and 19% above or below the PRL. In addition, they observed a variation in PRL size as determined by the locus of fixation stability.

1.4 Fixation Characteristics of the PRL

MD patients are usually able to perform smooth pursuit and saccadic movements from their PRL. However, their fixation performance is often compromised. Fixation performance is defined in terms of fixation precision and fixation stability. Fixation precision defined as the ability to repeatedly fixate at the same retinal locus while fixation stability as the degree of variability from the retinal locus while fixation is maintained (Schuchard, 2005).

In MD patients, eye movements made while fixating with the PRL have been observed to be different and mal-adaptive in comparison to eye movements made during normal foveal fixation. Crossland and Rubin (2002), demonstrated that fixation stability (defined as an elliptical area where 68% of fixation is held) at the PRL ranged from 0.2 to 0.5 degree in diameter for six patients. Schuchard (2005), using a similar method, also found fixation stability to range from 1 to 9 degrees in diameter in a study involving 1339 patients. This is a far cry from fixation stability at the fovea which is often within a degree (Schuchard and Raasch, 1992).

Poor fixation stability exhibited at the PRL has been accounted for by differences between peripheral and foveal vision. During normal fixation, the fovea is believed to direct the location of the target stimulus and also control drifts and micro-saccades in order to maintain fixation (Schuchard, 2005). These properties of the fovea are lacking at the periphery, and results in the higher saccade amplitudes and faster drift speeds observed in MD patients during eccentric fixation (Whittaker et. al., 1988). Thus the extent to which the PRL can assume the role of the fovea as a fixation locus is limited.

1.5 AMD and Vision Research

Cortical reorganization refers to the brain's ability to modify physical and functional neuronal connections in response to changes in experience. In the visual cortex, retinal lesions and other visual impairments that cause changes in sensory experience are factors that may yield adjustments of the relevant cortical neuronal circuits. The topographic relationship (figure 3) that exists between the retina and the calcarine sulcus in the striate cortex (McFadzean et. al., 2002) is another necessary factor conducive to the study of cortical reorganization. Studies in this area typically rely on electro-physiology and/or neuroimaging methods that directly or indirectly image the structure and function of the brain.

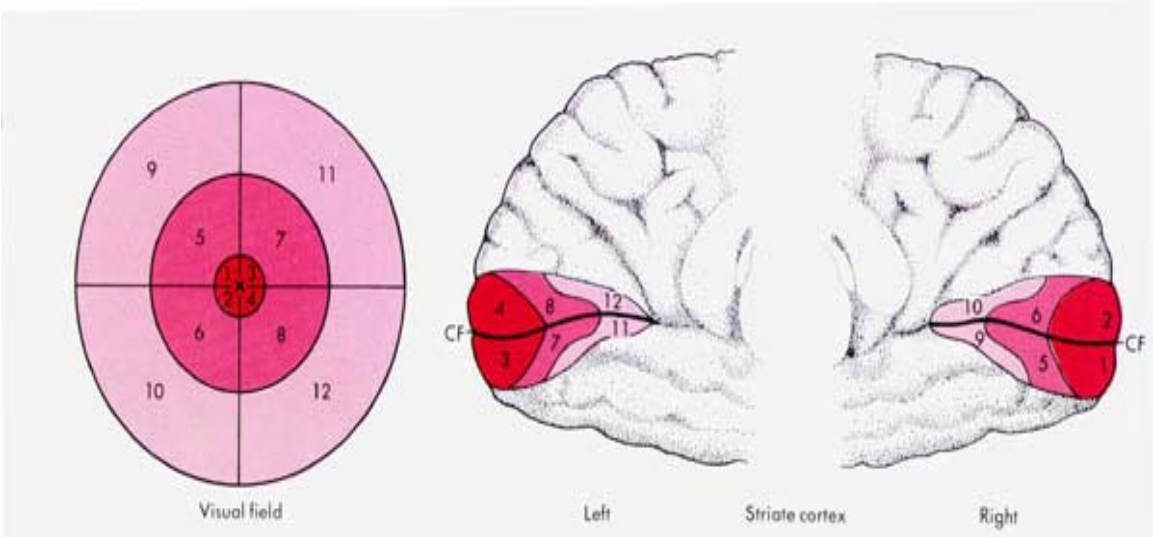

Figure 3: Topographic organization of the retina and the striate cortex

The central field of view occupies the majority of the striate cortex. Cortical area diminishes for locations in the peripheral retina.

In non-humans, research on cortical reorganization has been investigated using electro-physiological measurements from neurons in lesion projection zones – areas on the cortex deprived of retinal input as a result of topographically corresponding lesioned retina. Many studies report activity in the lesion projection zone to be initially absent after lesioning but to later resume with time (for example: Kaas 1990; Heinen and Skavenski 1991; Gilbert and Wiesel 1992; Darian-Smith

and Gilbert 1995; Calford 2000). These studies also report the resumed activity to be ectopic (i.e. elicited from retinal areas outside or adjacent to the lesion area). However, other studies investigating cortical reorganization in non-humans report a lack of evidence for the phenomenon. Murakami, Komatsu & Kinoshita (1997) and Smirnakis et al. (2005) for example used neuroimaging and failed to observed brain activity in the lesion projection zone.

Human research has also been conducted on cortical reorganization. The leveraging of MD populations to this inquiry has proven useful due to MD's pathology. Specifically, the presence of scotoma (Arroyo, 2006) and the use of PRLs as behavioral adaptations have been implicated as prime factors that yield cortical reorganization. These conditions make MD patients desirable participants for research into human cortical reorganization.

However, research with MD patients has provided no conclusive evidence to resolve the current inconsistencies in the literature. Baker et al., 2005 and Schumacher et al. (in press), for example, report evidence of cortical reorganization in MD patients while Horton and Hocking (1998) and Sunness et al. (2004) find no such evidence. It is uncertain what factors contribute to the present inconsistencies in the MD literature, but as MD creates abnormalities in the oculomotor system (Whittaker et. al., 1988) research attempting to detect long term cortical reorganization is most likely confounded by these abnormalities in eye movements (i.e. higher drift speeds and saccadic amplitudes).

Research on cortical reorganization in MD patients is typically conducted using fMRI. The equivocal findings described above may have resulted from the different levels of control exerted on the fixation instability of MD patients while in the fMRI environment (i.e. fixation instability may have been classified and corrected for differently across studies). Unfortunately, MRI compatible eye trackers provide only limited resolution to this issue. In fact, the fixation instability MD patients often exhibit overwhelms the eyetracker, preventing it from consistently locking onto their fixation

reference. An efficient way to account for fixation instability in MD patients in the fMRI environment is needed in order to advance neuroimaging investigations of cortical reorganization. A new technology, predictive eye estimated regression (PEER) is a potential solution for this problem.

CHAPTER 2: EYE TRACKING SYSTEMS

In vision research, eye movement and one's point of gaze are important behavioral performance measures and eye tracking systems are a long established measure of these attributes. Eye tracking systems have made possible quantitative assessments of ocular behavior and have led to significant insights into perception and cognition.

2.1 History of Eye tracking techniques

The first eye tracking system was developed in the 1900's to investigate reading. Huey, credited for this invention, used a lens (similar to a contact) with a hole for the pupil connected to an aluminum pointer that moved in response to the movements of the eye. His invention was followed by a non-intrusive eye tracker created by George Buswell. This device made use of light beams that reflected off the eye and onto a recording film.

Current eye tracking techniques include electro-oculography (EOG, figure 4I) and corneal reflection photography –a video-based system (figure 4II). EOG measures eye movement using electrodes pairs placed above and below or to the left and right of the eye. These electrodes measure the gradient in metabolic activity (potential difference) that exists between their respective positions around the subject's eye and in relation to the central resting position of the eye (Aslin and McMurray, 2004).

However, there are a number of limitations associated with EOG including variation of metabolic activity over time, high sensitivity to head motion, and the need for a pair of electrode for each axis of rotation. These limitations motivated the development of the corneal reflection photography based eye trackers. Corneal reflection photography is an eye tracking technique that uses infrared and near-infrared non-collumnated light to create a corneal reflection to provide contrast in locating the center of the pupil.

I  II 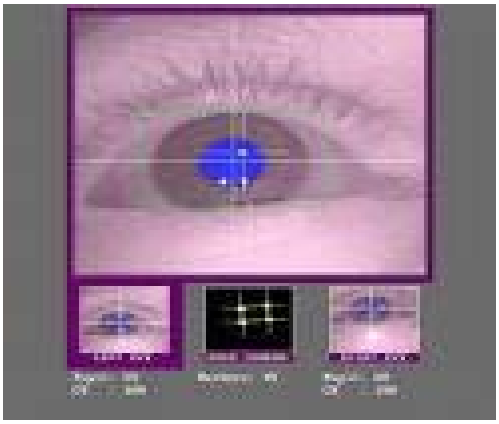

Figure 4: Electro-oculography (I) and Pupil-corneal reflection (II)

I: The figure above show eight electrodes one for each axis of rotation, one can see that this system is quite cumbersome.

II: In this figure, one sees the infra-red light reflected off the cornea and its position determined (in the bottom middle picture) by the eye tracker.

2.2 Eye tracker Applications

The eye tracker, as described earlier, is most often used to estimate point of gaze and eye movement. Applications of these measurements range from exploration of human psychology (scientific) to web usability and advertising (commercial). In advertising, for example, eye tracking studies are used to provide evidence for the effectiveness of a viewed product in terms of drawing and maintaining attention in magazines ads and television commercials. Alternatively, scientific applications of eye trackers enable the measurement of visual behaviors in humans within natural and experimental settings such as the fMRI environment.

Specific to the MRI environment are long range optic eye trackers. Long range optics allows MRI eye trackers to be positioned at most 16 feet away from the eye of the participant while they are supine within the scanner. The MRI compatible eye tracker optics is positioned to create an optical path from the eye tracking system (reflected off the stimulus display mirror) to the eye. Depending on the MRI application, a trade-off in sensitivity and cost usually exists. This tradeoff results from the expense of these highly sensitive eye trackers and the more expertise required for their operation.

2.3 Eye tracker limitations in fMRI

In the fMRI environment, ocular measurements using the eye tracker often involve several additional challenges; one of which is the eye tracker preparation process. Eye tracker prep in relation to the participant's eye and the scanning environment is a time consuming process that involves setting up an optical path to align infrared light to the cornea with no interference from the visual paradigm display. The presence of individual differences in the contrast of the pupil and the iris also makes the prep of MRI compatible eye trackers a tedious process. This issue is especially prevalent in subjects with dark pigmented irises as the eye tracker's ability to detect the pupil from the iris is limited by the reduced contrast between these two eye features.

Another challenge, specific to MD patients, is the MRI compatible eye tracker's limited sensitivity to detecting fixation. In normal sighted subjects, foveal fixation is very stable. These subjects maintain fixation on a visual target to within one visual angle of the target location. However in MD patients, PRL (eccentric) fixation is difficult to maintain at such high resolution. MD patients' fixation on a stimulus usually lies within 4 degrees of the target location (Schuchard, 2005). The fixation instability of MD patients often overwhelms the eye tracker's algorithms and prevents the system from consistently track the pupil. The unreliability of traditional eye tracking systems in relation to MD presents the need for an alternative approach. Accurate measurement of eye positions during eccentric fixation is crucial in neuroimaging studies of macular degeneration.

CHAPTER 3: PREDICTIVE EYE ESTIMATION REGRESSION

Challenges to determining eye positions of MD patients during neuroimaging have led to the development of alternative measuring tools (PEER). A few basic criteria must be met before any eye tracking approach can be considered viable. First, the alternative eye tracking system must efficiently and accurately obtain eye position and eye movement measurements. Second, the system must be insensitive to the individual differences in fixation. Third, the alternative system should incur minimal monetary or timely cost.

3.1 Predictive Eye Estimation Regression (PEER)

PEER is an MRI based alternative eye tracking approach (LaConte, 2006) that makes use of a supervised learning method called Support Vector Machines (SVMs). The SVM is the workhorse of the PEER algorithm. It relies on training data consisting of input vectors (x_t) and their corresponding targets (y_t) at a time point t. The input vectors are the intensity measurements of brain voxels in slices (in any orientation) through the eyes (figure 5), while the corresponding targets are the positions of the presented stimulus during the visual task at particular time points (figure 6) (LaConte, et. al, 2003). Hence, for each stimulus position presented on screen there is a unique spatial intensity pattern generated in the brain. SVM makes use of the relationship between these two datasets (training dataset) run to predict future points of gaze of each participant.

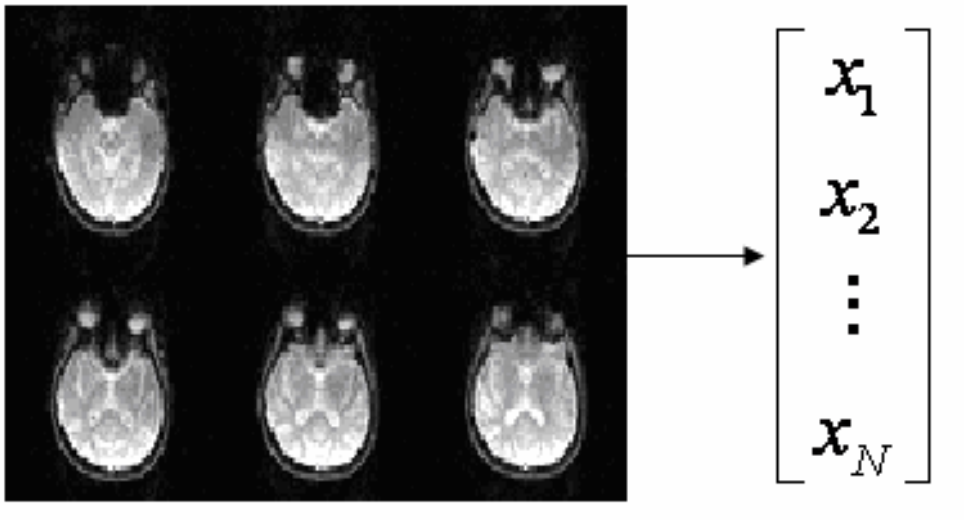

Figure 5: Data Representation (Example Input Vector)

In the axial slices above the measured brain voxels represent the input vector, where N represents the total number of voxels measured at time point t, of the training data.

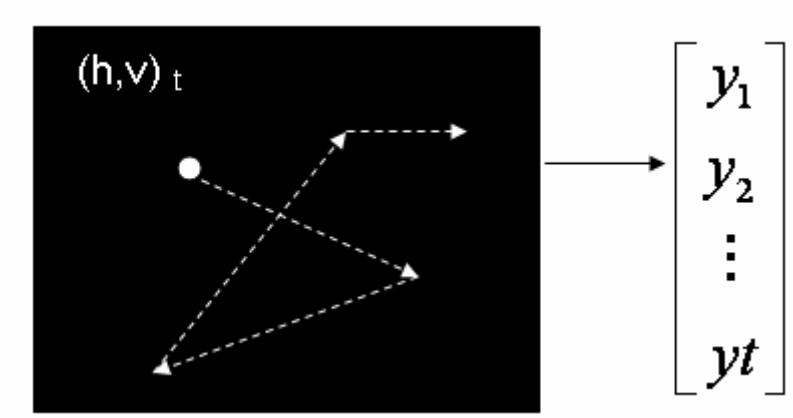

Figure 6: Data Representation (Targets)

In the figure above $(h, v)_t$ represents the x and y coordinates of the target stimulus, at time point t, on the visual display. However, it should be noted that the sequence of position on screen above is not the actual sequence used during the calibration run.

PEER requires a calibration run to establish a trained model. The calibration run can be acquired at anytime during an experimental session and as many times as desired. The trained model, estimated from the calibration data, determines the participant's point of gaze in subsequent fMRI runs (the testing dataset). This calibration setup (figure 7), allows the trained model efficiently

represent each participant's fixation characteristics throughout the experiment and improves the model's sensitivity, accuracy and efficiency in determining fixation gaze.

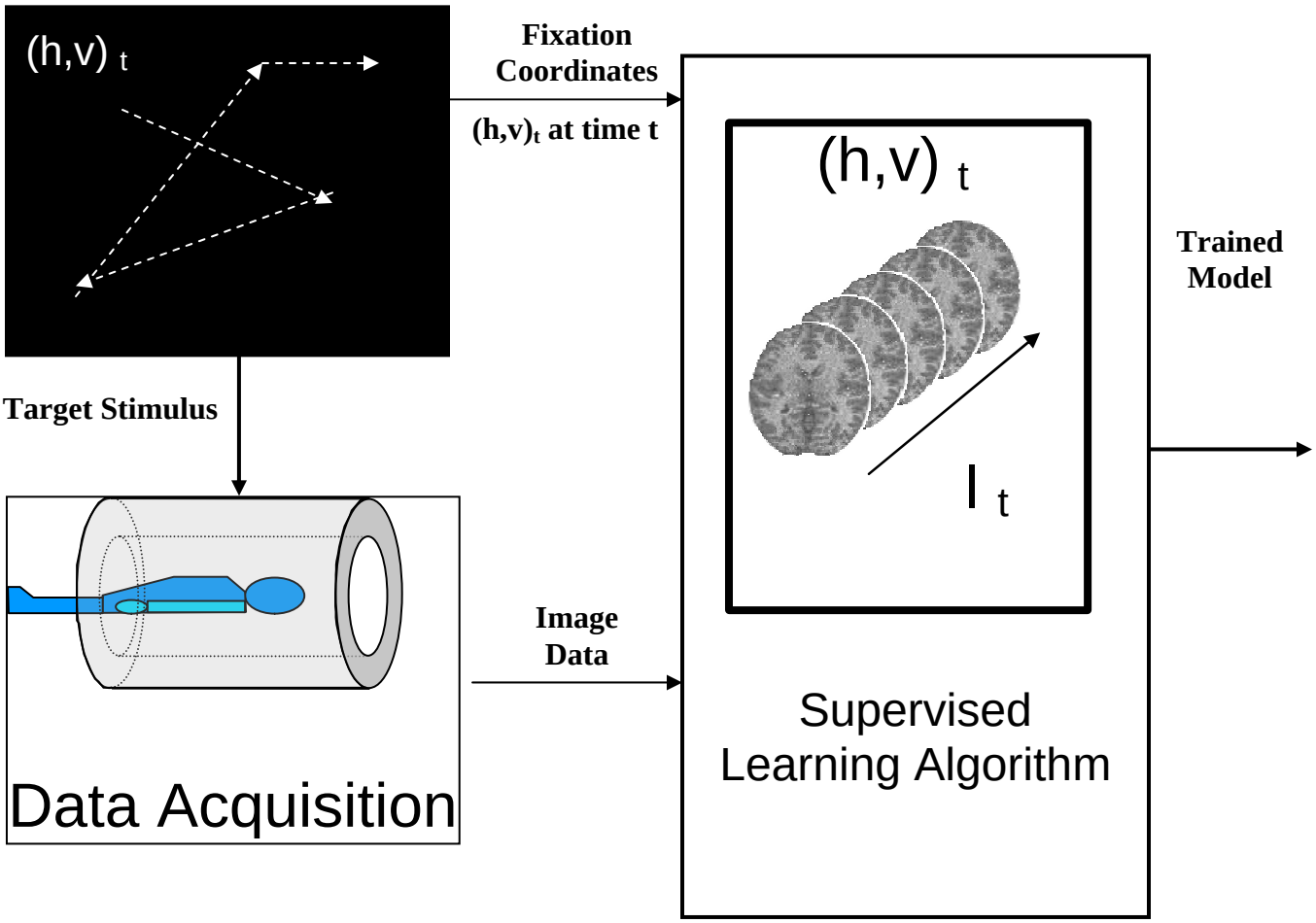

Figure 7: Calibration (Model Estimation)

The diagram above (courtesy of LaConte, 2006) provides an outline of PEER's algorithm. As seen above the fixation coordinates as well as the image data is fed into SVM where a model is estimated.

3.2 PEER: The MR Signal

PEER's MR signal is affected by two interdependent parameters: repetition time (TR) and scanned brain volume or coverage. These parameters affect the signal to noise ratio (SNR) achieved during experimentation. Thus to obtain the optimal SNR in PEER, optimal values for these two parameters were researched. The optimal values were determined by varying the TR between 126ms and 251ms and the scanned brain coverage between four and eight slices.

The TRs above were chosen to match the temporal order at which MD patients execute eye movements. In McMahon et al., (1991) MD patients were reported to have gaze duration of about 250 – 350ms. Thus the TRs were kept below or within this range. In addition TRs with higher time intervals below or within this range were favored because of the increased MR signal they produce.

The specific TR and the number of brain slices scanned were determined by the scanner hardware limitations. For example gradient strength, a scanner parameter, determines the number of slices that can be scanned in a time interval. Thus in obtaining PEER's optimal parameters, TR was the primary variable and scanned brain slices a consequence of the chosen TR.

The TE duration was also short in order to eliminate the T2 effect and thus remove differential signal strengths (in the different tissues). The short TE was also used to yield greater image contrast and greater signal strength. The PEER image obtained was T1 weighted. Altogether, the optimal TR and hence scanned brain slices were chosen to provide an appropriate balance between SNR and the fixation characteristics of MD patients.

3.3 Support Vector Machines (SVMs)

SVMs are statistical supervised learning tools used for data classification and regression. The term "supervised learning" describes the machine's need for training data in order to predict future response values to a set of inputs. SVMs arise from Vapnik's Statistical Learning Theory (Vapnik, 1995).

PEER data falls into the class of suitable SVMs applications because of its small sample size (time) and high dimensional input (space) (LaConte et. al, 2006). PEER uses Support Vector Regression (SVR) to predict point of gaze. SVR creates a function based on the training dataset $\{(x_1, y_1)\ldots (x_n,y_n)\}$, where x denotes input vectors and y the scalar targets given. In PEER, this training set is obtained during the calibration routine. The calibration routine consists of the input voxel

intensities (x_i) from the scanned brain slices at a particular point in time (i) and the corresponding stimulus position in visual field degrees ($y_{i,}$) .

The function estimated by SVR should have at most ε deviation from the actual targets (i.e. the subject's points of gaze during experimentation). In PEER, ε was chosen to be 0.001. The SVR estimated function should also be as flat (linear) as possible (figure 8, for more details on SVR see Smola, et. al, 2003). The function to be estimated can be described in linear terms as:

$$f(x) = \langle w, x \rangle + b \tag{1}$$

with b the intercept, w a vector of the same dimension as x, and <·,·> a vector product. Also w can be described as a linear combination of a set of the training inputs (x_i) –the support vectors. The flatness of the function is ensured by seeking a small w. This is done by minimizing its norm i.e.

$$\|w\|_2 = \langle w, w \rangle \tag{2}$$

In mathematical terms, this problem of achieving as much flatness as possible and restricting output deviation to within ε is called a convex optimization problem. In finding the solution to w the following equations are solved:

$$\left\{ \begin{matrix} yi - \langle w, xi \rangle - b \le \varepsilon; \\ \langle w, xi \rangle + b - yi \le \varepsilon \end{matrix} \right\} \tag{3}$$

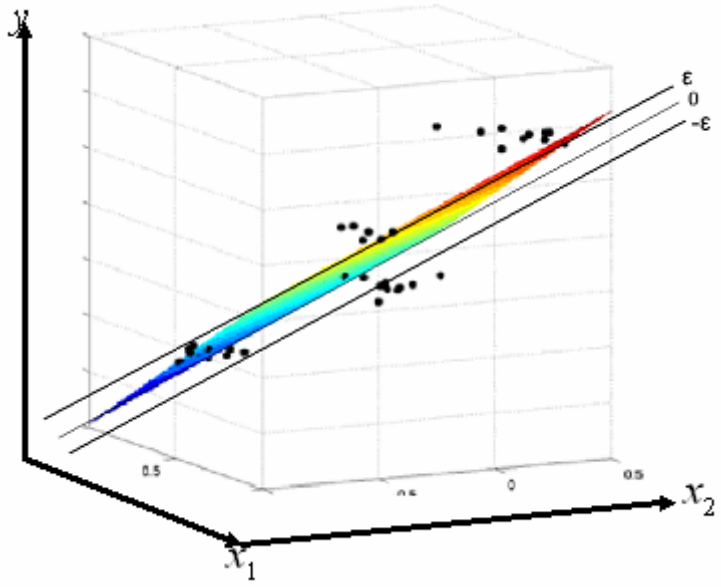

Figure 8: Temporal Regression (a 2D input vector example)

The figure above shows the regression performed by SVM. X1 and X2 represent the input vector (**x**) fed into the machine and Y the targets (in our case point of gaze) at each time point t. The deviations from the regression line (slope) to the targets on both sides make up ε. ||w|| (specifically ½(||w||^2), defines the length of the function to be minimized. Also in this figure b is zero.

The assumption for the equations above is that the estimated function is an optimization problem feasible with ε precision. However, as this is not always the case. A "soft margin" loss function (Bennett and Mangasarian, 1992) is incorporated into both equations above by introducing slack variables (ξ, ξ*).

Thus the $\|w\|^2$ in equation (2) becomes $\frac{1}{2}\|w\|^2 + C\sum_{i=1}^{l}(\xi_i + \xi_i^*)$ (4)

and the optimization problem in equation (3) becomes:

$$\begin{Bmatrix} yi - \langle w, xi\rangle - b \le \varepsilon + \xi i; \\ \langle w, xi\rangle + b - yi \le \varepsilon + \xi i^* \end{Bmatrix} \quad (5)$$

provided $\{\xi_i , \xi_i^* \ge 0\}$ (Vapnik, 1995).

In equation (4) C determines the trade-off between the flatness of the function and its deviations greater than ε. In PEER, C was chosen to be a 100. This C value was chosen from investigations reported in LaConte (2005) on the relationship between C and its effect on function prediction (see fig 4 in LaConte, et. al 2005).

In applying the SVR theory to PEER, SVM^{light} an implementation of Vapnik's Support Vector Machine in C (Joachims, 2002a, Joachims, 1999a) was modified to handle fMRI image data and used for regression analysis on the training and testing datasets. SVM^{light} is a high performance software that has been used in a large range of problems, including text classification (Joachims, 1999c, Joachims, 1998a), image recognition tasks, bioinformatics and medical applications.

CHAPTER 4: CURRENT STUDY

MD patients are unable to maintain stable fixation and often use multiple PRLs. These deficits prevent the localization of measured brain activity in fMRI and impede our ability to accurately measure the location and degree of cortical reorganization in the primary visual cortex. This current study proposes to create an fMRI compatible algorithm to help control for fixation instability by estimating point of gaze.

4.1 Determining Fixation Instability

Previous research by LaConte et al (2006), has shown PEER as an alternative approach for accurately estimating point of gaze in normally-sighted subjects. In the current study, PEER is used to determine fixation instability in MD patients. In determining fixation instability, PEER was divided into two phases. The first phase was used to determine PEER's optimal parameters and the second to determine fixation instability. This first phase was necessary for PEER to efficiently estimate point of gaze specific in MD patients. In the second phase, point of gaze estimates and fixation instability classifications were made for each participant. Data were collected on a normally sighted and two MD patients.

4.2 Limitations and Compensations

PEER depends on the amount of information present in the training data set- the calibration routines. Therefore, a tradeoff between the length and the amount of calibration routines presented and PEER's robustness was considered. The short TRs used required a fast imaging acquisition method and a multi-channel head coil; however the TRs provided PEER with a high sampling rate suitable for measuring minute changes in the eye. The absence of a traditional eye tracking system in the scanner is another limitation. This limitation prevents the comparison of PEER to eye tracking data within the same time frame. PEER's validity was determined by comparing its estimations and the MP-1 results of both MD participants and the control participant in all visual tasks.

CHAPTER 5: METHODOLOGY

5.1 Participants

Three participants participated in this study – two MD patients and one normally-sighted control participant. All participants gave informed consent and were compensated for their participation. The two MD patients were recruited from the Emory Eye Clinic. They both developed MD in adulthood and have lived with the disease for less than ten years.

The MD patients met several eligibility criteria. First, neither was completely blind. Both had residual vision in their periphery. That is, their retinal damage was within 3,000μm radius of the fovea. Second, visual acuity in each patient was better than 20/200. Third, both patients had a dominant PRL (i.e. the PRL with better visual-function capability) and were able to fixation within this dominant PRL for 30 seconds or more. Finally, all participants were screened for other visual deficits (e.g., cataracts, glaucoma, etc.). The table below provides information about the visual health of all participants.

Table 1: Participant Demographics

Participant	Group	Age/Sex	Time since Onset	Eye Used
JR	AMD	78/F	R: ~ 2 yrs, L: ~ 6 yrs	Right
RD	AMD	71/M	R: ~ 2 yrs, L: ~ 2 yrs	Left
TA	Control	23/F	N/A	Both

Time since onset is approximated in the table. The values given above reflect the time of diagnosis as the actual onset of disease is likely to have occurred before diagnosis. The eye used indicates the eye with the best visual acuity. It was identified for each participant and was used in subsequent phases of the experiment (e.g. MP-1, fMRI).

5.2 Apparatus

An MP-1 microperimeter (Nidek Inc.) and a Siemens 3T magnet were used in this study. The MP-1 was used to identify and map the extent of scotomata. It was also used to determine the dominant PRL based on a fixation test. The Siemens 3T scanner was operated inline with the PEER algorithm to collect MR signals used to determine point of gaze and fixation stability.

5.2.1 Perimetry

Perimetry is a systematic measurement of the retina's sensitivity to light by the detection of test targets on a defined background. The whole visual field is tested by presenting a test target at different luminance values at random locations on the retina.

The MP-1 was used to perform perimetry via the fundus tracking method. This real-time eye tracking system of the MP-1 allowed accurate determination of eye position despite eye movements. The eye tracking system worked by first establishing a reference point, a biological landmark on the retina (usually a bifurcation of the blood vessels), and then collecting infra red images continuously throughout the exam. All results obtained from the MP-1 were registered onto a digital fundus photograph for qualitative assessment of retinal sensitivity and the degree of fixation instability.

5.2.2 MRI

Functional MRI was used in the second phase of this study. The scanner used was a Siemens 3T Magnetom TrioTim system with up to 102 seamlessly integrated coil elements and 32 RF channels. The scanned images were obtained using an echo-planar sequence and collected at a flip angle of 18 degrees. The image slices were scanned through the participant's eyes, in the transverse plane, 4.0mm in thickness, with a base resolution of 64 voxels and a voxel size of 4.0 x 4.0 x 4.0mm. In addition, because of the short TRs tested, a multi-channel head coil that supports the GeneRalized Autocalibrating Partially Parallel Acquisition (GRAPPA) fast imaging method was used.

A structural image was also collected for each participant in the experimental protocol. The structural image was scanned in the sagittal plane using a fast echo-planar sequence. A TR of 2600ms, a TE of 3.02ms at 8 degrees flip angle was used. The structural image was also scanned in GRAPPPA mode. The scans had a base resolution of 256 voxels and a voxel size of 1.0 × 1.0 × 1.0 mm. A total of 176 volumes were collected. Structural scans lasted 4 minutes and 7 seconds.

5.3 Visual Stimuli

In both the MP-1 and the 3T scanner the visual stimuli presented to each participant was manipulated to compensate for the participant's visual acuity and extent of the central scotoma. Stimulus parameters such as size, location, and contrast were set on the visual paradigm to compensate for individual differences in retinal function.

5.3.1 MP-1 Visual Stimulus

The MP-1, during perimetry, made use of a 76 Goldmann III stimulus (white, circular light). This stimulus was displayed at different luminance values based on a logarithmic scale ranging from 0 dB, the brightest stimulus (127 cd/m^2), to 20 dB, the dimmest stimulus (1.27 cd/m^2). Stimuli were randomly presented, within 20 degrees eccentricity of the visual display, in a dense to coarse sampling protocol from the center of the retina to the periphery. The stimuli were also presented in a sequence and spaced approximately 2 degrees apart in the visual field.

The retinal maps below (figure 9) exemplify the data to be obtained on retinal sensitivity and fixation stability of each participant during perimetry. In figure 9(II) the sampling protocol used in presenting the stimulus is illustrated. The bigger sections represent the less densely sampled areas in the visual field while the smaller sections the more densely sampled areas. The term sampling describes the points in the visual field at which the stimulus is presented. The number on the sections show the sequence in which the stimulus was presented and the color code a qualitative assessment

of retinal sensitivity per section –the lighter the color the higher the retinal sensitivity of that area. The color code is labeled according the stimulus luminance intensity at which a participant responds.

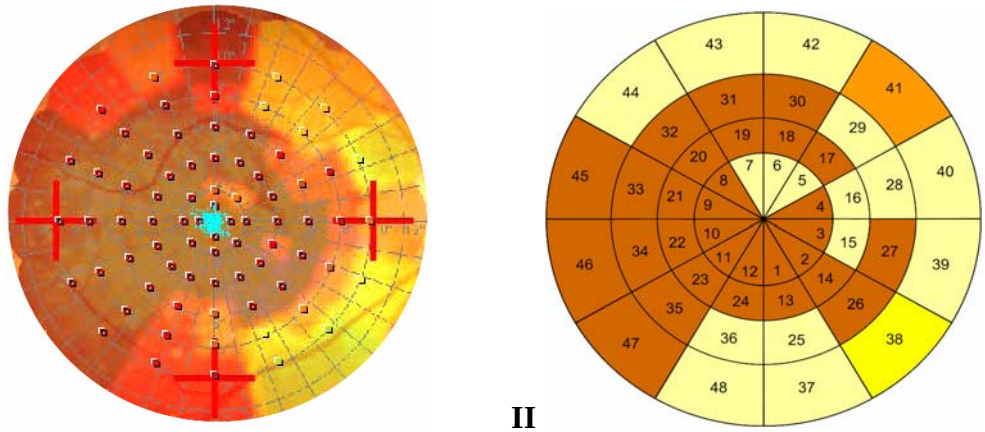

Figure 9: Symbolic Retinal Map (I) and Color-coded section (II)

Scotoma sections are in brown. Section 38 (yellow) is the PRL. In the brown sections on the map, the stimulus was presented at its brightest and at reduced stimulus luminance values in the lighter areas.

Kinetic perimetry was also performed to determine the boundaries of retinal sensitivity (i.e. the extent of the scotoma) in the visual field. The test used the same 76 Goldmann III stimuli however the stimulus moved from the center to the edge of the visual field until detected by the participant. The stimulus intensity was chosen according to the protocol used in standard perimetry.

A fixation test was also conducted. This test was divided into two phases: a single cross (PRL) fixation test and a four cross (foveal) fixation test. In both fixation tests the crosses used were red in color and presented over a homogenous gray-black background.

The single cross fixation test involved participants fixating at a single cross placed at the center of the visual display. The four cross fixation test, however, tested fixation stability at the fovea using four crosses placed at locations corresponding to the preserved peripheral areas of each participant's retina. In the control participant, these two fixation tests were assumed to elicit use of the same retinal fixation reference (i.e., the fovea).

5.3.2 MRI Visual Stimulus

For presentation in the 3T scanner, a visual graphic software called Vision Egg (Straw, A.D., et al., 2006) was used to design the stimulus. Contrast and stimulus size were used to compensate for reduced visual acuity and fixation instability in MD patients. In all eye movement tasks, a flashing white circle with a flash frequency of 8Hz was used as the stimulus. The stimulus was also contrast enhanced by being displayed over a homogeneous black background (figure 10).

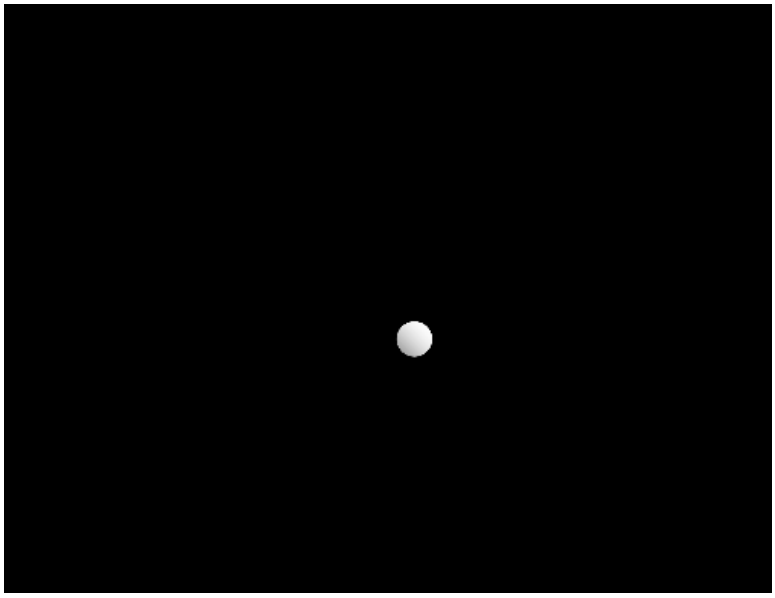

Figure 10: Visual stimulus of eye movement tasks

The stimulus used in all eye movement tasks. The white circle at the center flashed at 8Hz.

The calibration routine made use of the stimulus above (figure 10). This stimulus was first presented in a primary position of gaze (center of the screen) for 6 seconds. Next, it appeared in one of nine randomly chosen secondary positions of gaze (any vertical, horizontal or oblique deviation from the primary position of gaze) for 6 seconds. In a single calibration run this stimulus presentation sequence occurred twice for a total of 38 stimulus presentations.

In Schuchard (2006), MD participants were observed to use a different PRL to fixate when the stimulus was randomly placed at a secondary position of gaze. This effect was minimized in the calibration run with a stimulus sequence that constantly varied between the primary position of gaze

and the randomly selected secondary position of gaze. This sequence was used in order to "reset" the PRL used by the MD participant to the dominant PRL that is mostly used for fixation at the primary position of gaze.

In the smooth pursuit task, the same stimulus was used. It was however mobile, randomly moving along the vertical, horizontal or diagonal (left/right) axis. These two stimulus features were programmed in vision egg using mathematical equations to represent change in direction and distance. The rate of change in distance was 10 degrees per second. At the start of the smooth pursuit task, the stimulus appeared at the center of the visual display for 10 seconds. Then, the stimulus began to move in a random direction. The stimulus moved back and forth within a specified boundary of 16.5 degrees in the horizontal direction and 12.6 degrees in the vertical direction. A complete cycle in the selected direction involved the stimulus moving from the center to the positive and negative ends of the boundaries and back to the center. The stimulus direction was then reset to the center and the next direction randomly chosen after a total of 12 cycles occurred in the current direction.

A random fixation task was also conducted. This task used the same stimulus as in the calibration routine however the stimulus was presented at random positions on the visual display throughout the task. The boundaries at which the stimulus was presented were identical to that in the smooth pursuit task. Stimulus randomization was done using a built-in function in vision egg.

In the fixation tests, the target stimulus (a white cross) was displayed over a black background. Fixation on the cross was enhanced with a small but visible flashing white circle placed at its center. The flash frequency of the circle was altered across test blocks to boost participant fixation. The flash frequency was programmed to vary between either 2Hz or 4Hz in the single cross test and either 2.5Hz or 4.5Hz in the four cross fixation test. In addition, the placement of all four crosses was varied across participants to ensure that each appeared outside the scotoma. They

appeared at 10 degrees for the control. Verbal instructions were given in all experimental tasks to compensate for the reduced visual acuity in MD patients.

5.4 Procedure

The data collected from each participant included best corrected visual acuity in the best diseased eye. Contrast sensitivity, the ability to discern between luminosity levels in static images, was evaluated in all participants using the Mars Letter Contrast Sensitivity test. The chart determined the contrast required to read large letters of a fixed size by varying the contrast level across the chart. Color sensitivity was tested by having participants arrange an array of colored disks- the Farnsworth Dichotomous Test. The result from the Farnsworth test showed all participants have normal color discrimination. The table below details the visual acuity and contrast results of the ophthalmologic exams.

Table 2: Ophthalmologic Exam results

Participant	Visual acuity	Contrast
JR	20/100 (Right)	1.20
RD	20/160 (Left)	1.20
Control	20/20 (Both)	1.68

Visual acuity scores are standard Snellen fractions. Normal contrast scores in the older adults range from 1.6 to 1.7, where a higher score indicates better contrast sensitivity.

MP-1 tests followed these basic visual tests. The MP-1's fixation test results were used in classifying fixation stability as: stable if 75% of the fixation positions reside within two degree diameter circle, as relatively unstable if more than 75% of the fixation positions reside within four degree diameter circle and less than 75% fall within the two degree circle; and as unstable if less than 75% of the fixation positions are within the four degree diameter circle. After MP-1 testing participants were escorted to the scanner for the fMRI phase of the study. Participants were then placed supine in the scanner with their head secured within the multi-channel head coil. Their

comfort was ensured. A patch was placed over the participant's eye with worse vision. The participant was then instructed about the task, via a two way intercom.

The MRI phase of the experimental protocol involved two stages. In the first stage, the optimal PEER parameters were acquired. The scanned brain volume and TR were varied to establish PEER's optimal parameters. Data were collected from a normally sighted participant tested on two smooth pursuit tasks. The results from this stage were applied to the second stage, in which, each participant's point of gaze was estimated during eye movement and fixation tests.

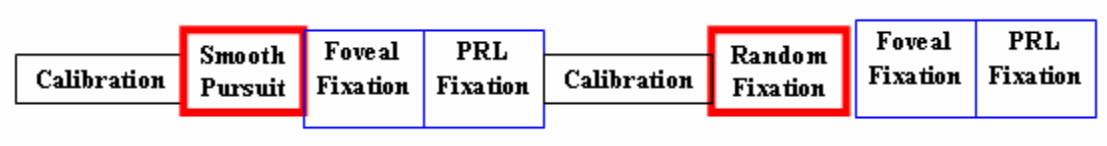

Figure 11: fMRI Experimental Design (participants 1-3)

This sequence of experimental runs was repeated three times to make up one experimental session with a time duration of 45mins.

A blocked experimental design (figure 11) was used in the second stage. This design was repeated three times in the scanner. The duration of each task varied. The first block was the calibration routine. It lasted 3 minutes and 8 seconds. The next block was the smooth pursuit task. It also lasted for 3 minutes and 8 seconds. The fixation task followed with the single cross (PRL) fixation first and then the four cross (foveal) fixation. In the single cross fixation test participants were instructed to fixate as they naturally would (i.e. with their dominant PRL) on a single cross. In the four cross fixation test, participants were instructed to focus on the four cross in such a way that their central visual area or scotoma was placed within the four crosses. Both task lasted for 30secs. A random fixation task, which lasted for 60secs, was also included in the experimental session.

Task performance was evaluated and improved by participant suggestions. In the eye movement tasks, for example, all participants were able to detect and follow the stimulus. However in fixation test, the flash frequency of the circle at the center of the cross was increased to aid fixation (to the frequencies mentioned above) due to suggestions from the first MD participant. This flash frequency was used on subsequent participants.

CHAPTER 6: DATA ANALYSIS

6.1 MP-1 Data Analyses

Data collected from the MP-1 consisted of a visual map of the scotoma, as well as point of gaze estimations for both fixation tests. In all tests, each participant's fixation position was plotted as a line graph and scatter plots. These plots were used to classify fixation stability in each participant.

6.2 PEER Data Analyses

Data were collected from fMRI slices through the eyes of each participant. All scanned slices were referenced to the middle axial slice through the eyes (figure 12) in all the tasks.

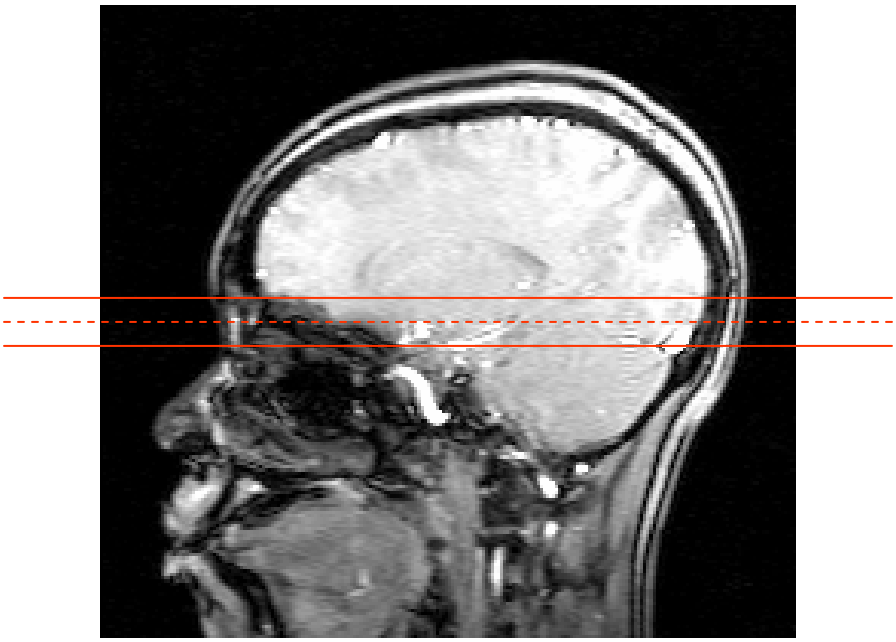

Figure 12: Region of Interest across eye sockets

MRI 3D anatomical image with red line indicating the slices scanned during the calibration routine and the other experimental tasks.

Data preprocessing was done in AFNI, Analysis of Functional Neuro Images. The data (DICOM files) were first converted into AFNI format. Next, head motion was corrected in the images by registering all the scanned slices from all the task runs to the first scanned slice from the first calibration run. These alignments were done using Fourier interpolation and the motion results

were printed in terms of roll (rotation about the inferior-superior axis, pitch (rotation about the right-left axis), and yaw (rotation about the anterior-posterior axis). Finally, the motion corrected data collected during the calibration phase was concatenated in order to obtain a collective training data set for input into SVM.

A measure of standard error was used to interpret the results from PEER. The root mean square of the absolute difference between each PEER estimated fixation position and the stimulus positions presented during each task were used in calculating the standard error. The absolute difference was used in order to eliminate the positive or negative direction of the difference in the standard error. The standard deviation from the standard error (across all fixation positions) was also calculated in each task block.

The analyses on all tasks were separated into horizontal and vertical components and all variance estimates were used in classifying each participant's fixation instability. Fixation instability was classified as: stable if standard deviation was less than 2 visual field degrees, relatively unstable if the standard deviation was between 2 -4 degrees and unstable if greater than 4 degrees. Figure 13 (below) illustrates the procedure used in calculating the standard error and standard deviation. In the four cross fixation test, all PEER's position of gaze estimates was compared to the stimulus position at the center of the screen.

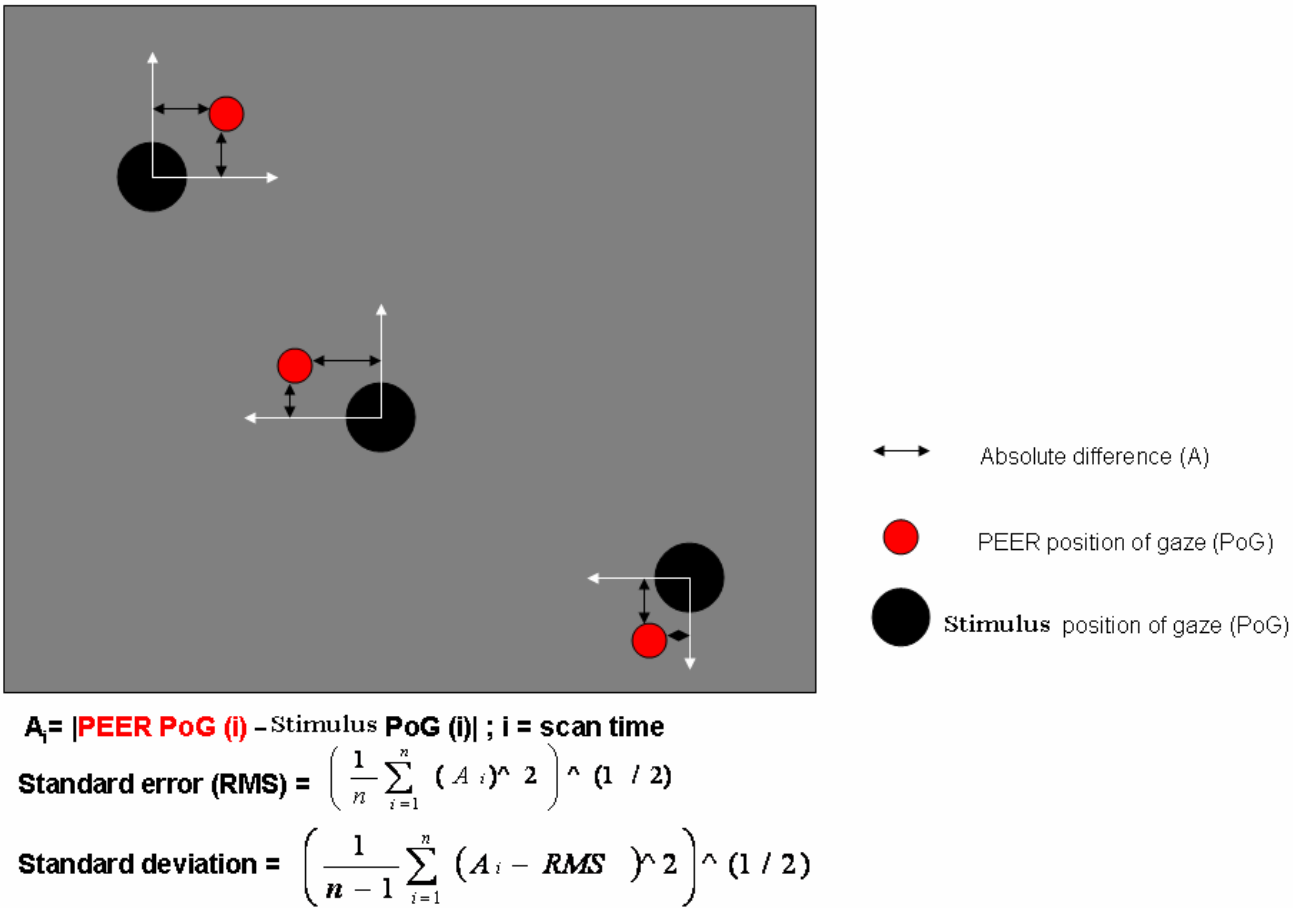

Figure 13: Calculating standard error and standard deviation (Illustration)

A Levene test for equality of variances was used to test the differences between the variances obtained from each TR in the first experimental stage as well as in the fixation tasks presented in the second stage. In the first stage, the results from this test were used to establish a valid choice of the optimal PEER parameters. In the second stage, the test allowed for comparisons between the single cross (PRL) fixation test and the four cross (foveal) fixation test in each participant.

CHAPTER 7: RESULTS

7.1 MP-1 Perimetry results

The perimetry exam was conducted on each MD patient's better functioning eye and on both eyes for the control participant. It was observed that the dominant PRL chosen by each MD participant did not always correspond to the area with the highest retinal sensitivity. The following figures display the perimetry results for each participant. The red sections represent dense scotomata. The lighter colors (with dark green being the most sensitive) represent functional retinal areas. in terms of retinal sensitivity. A white circle is used to locate each participant's PRL on the retinal map.

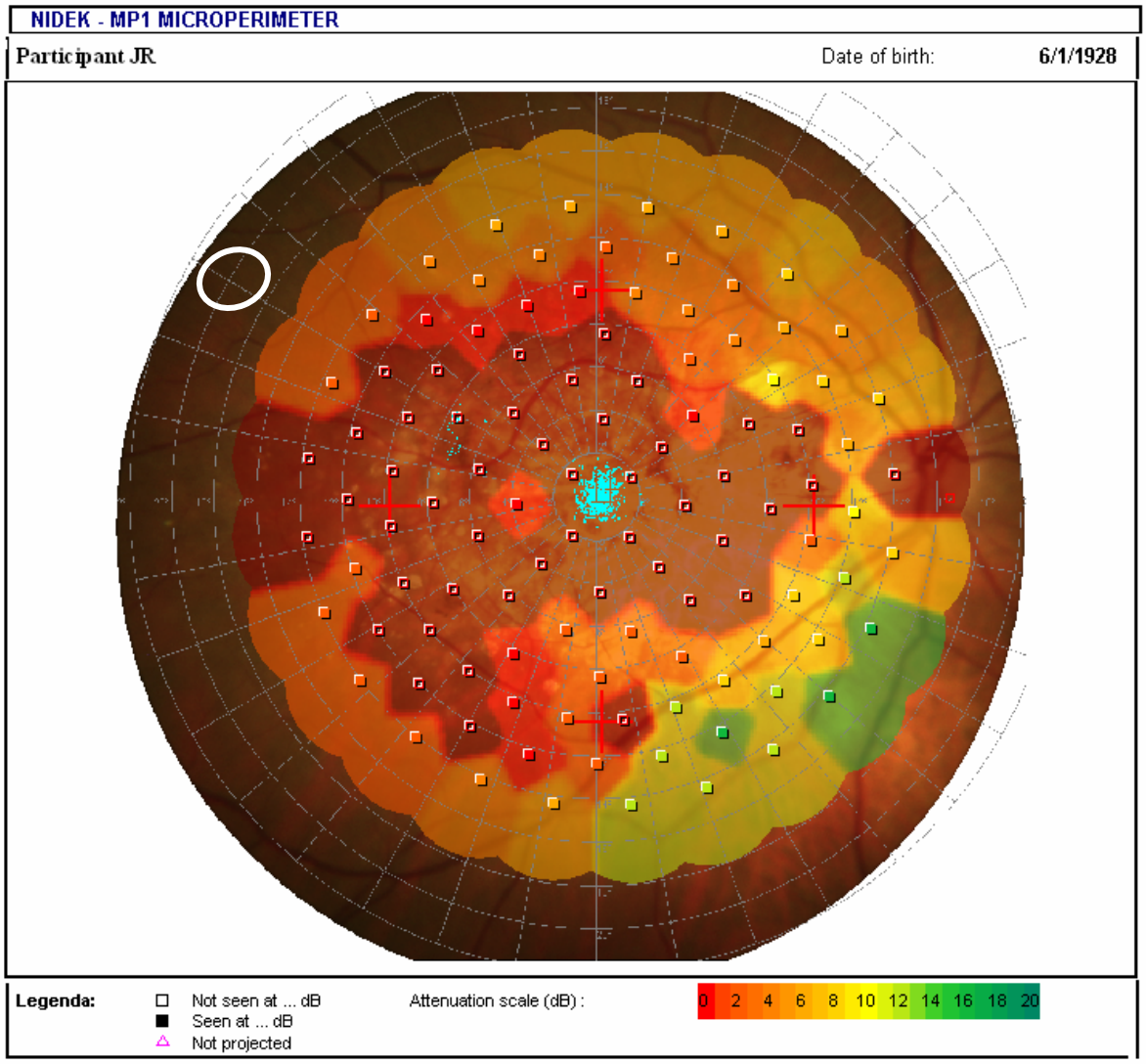

Figure 14: Participant JR's Retinal Map

The high retinal sensitivity present in the bottom right visual field suggests that participant JR might eventually develop a dominant PRL in this quadrant. However, at this time of testing, participant JR's dominant PRL is located at the upper left quadrant (see figure 16).

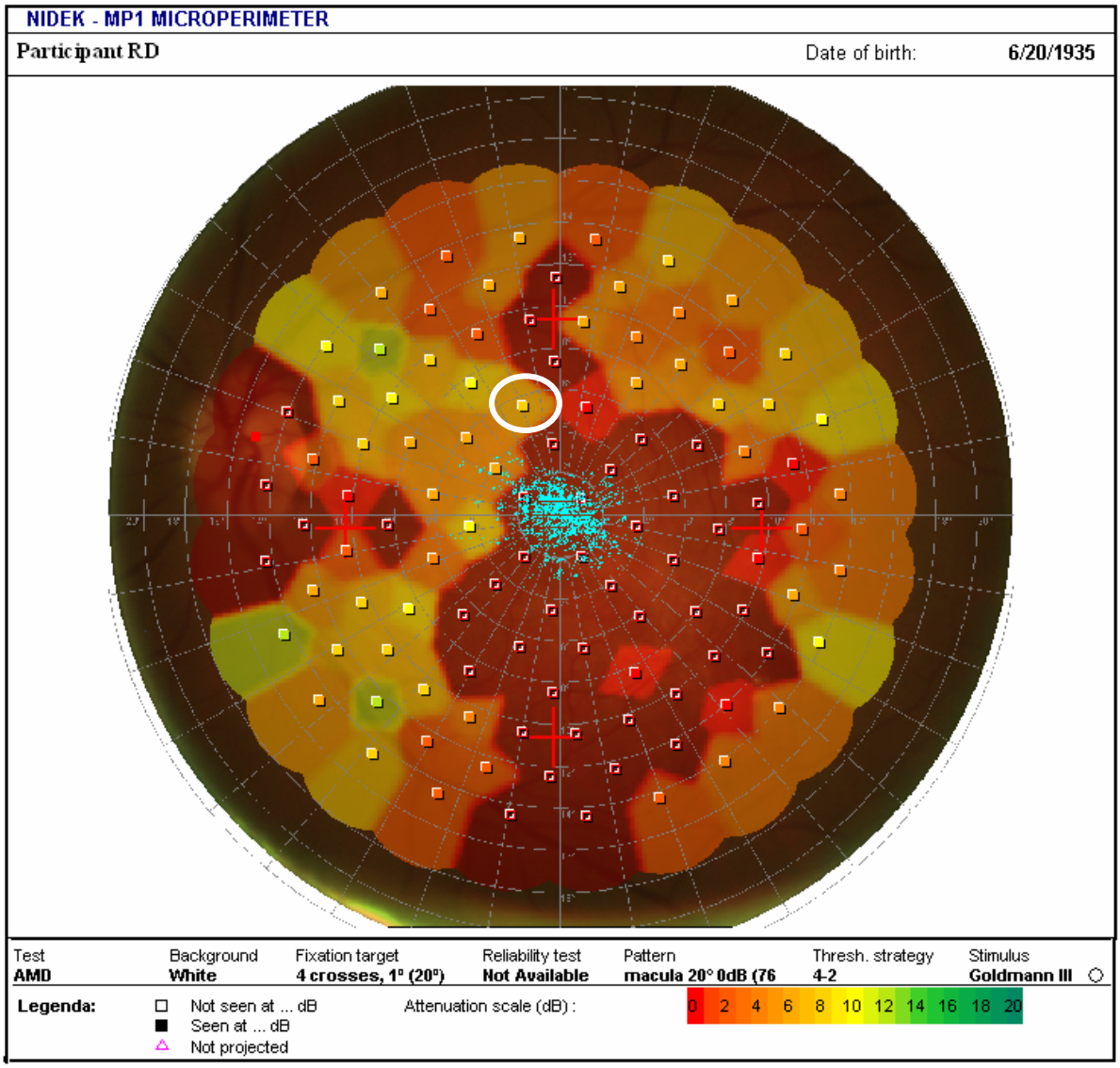

Figure 15: Participant RD's Retinal Map

In the figure above, participant RD's difficulty in fixating during the perimetry exam is seen. Fixation in this test was classified as relatively unstable by the MP-1 and is most likely the result of the little or no retinal sensitivity at the locations the four crosses were placed. Participant RD's PRL is located at about 4 degrees above the fovea and has a retinal sensitivity of 8dB.

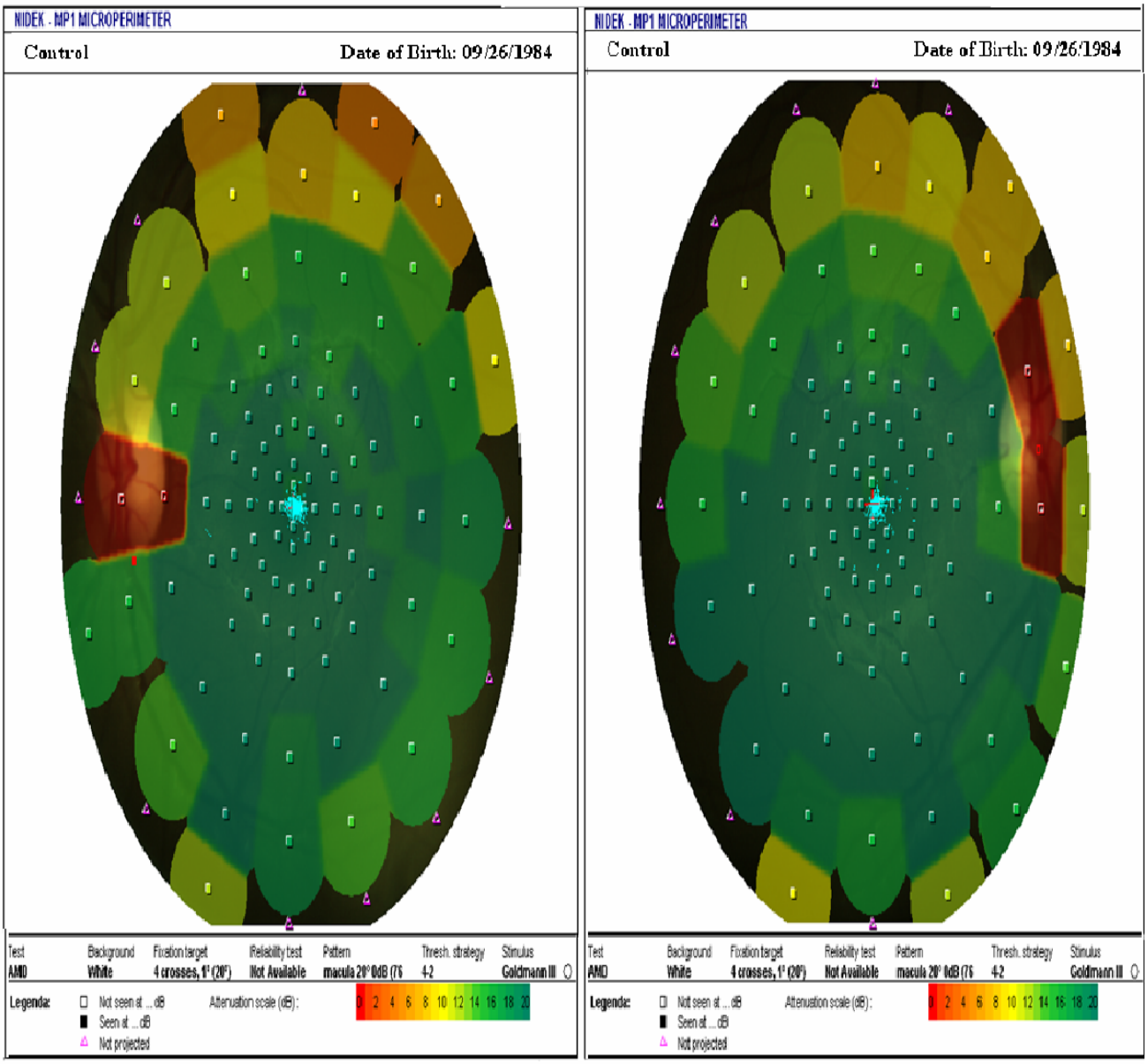

Figure 16: Control participant Retinal Map (Left eye and Right Eye)

The perimetry results above show the control participant with a normal sensitive retina. Retinal sensitivity at the fovea was observed at 20dB while most peripheral areas were within the range 8 – 20dB. On both images, one can see that no sensitivity to light is present at the optic nerve. The figure also shows the control participant's steady fixation at the fovea throughout the exam.

7.2 MP-1 Fixation results

The fixation test was done twice, once while each participant fixated a single cross with their PRL and again while they fixated with the four crosses. The figures below show the fixation pattern of each participant (note: participant RD was unable to perform the four cross fixation test) during both fixation tests.

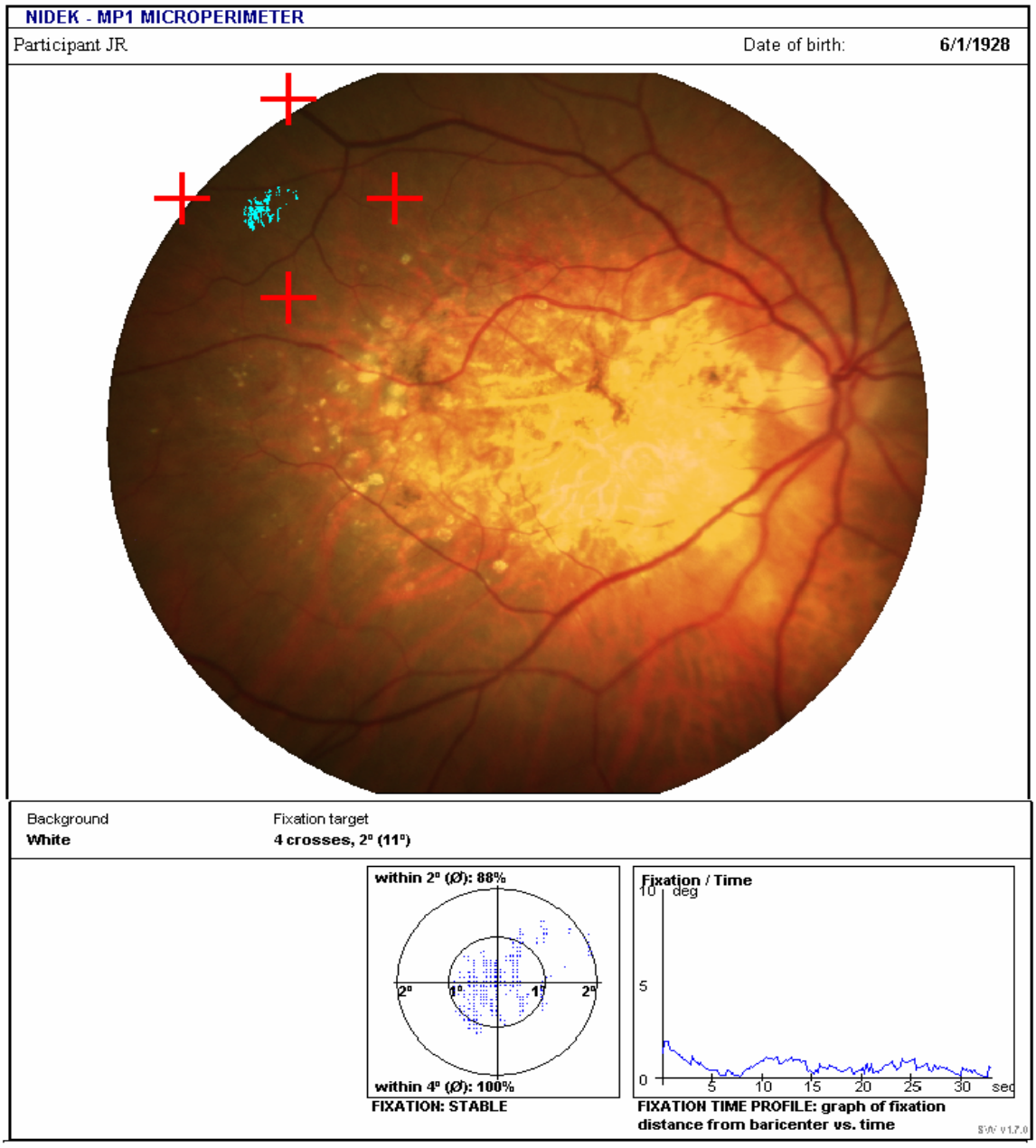

Figure 17: JR MP-1 single cross fixation test

In the figure above, participant JR's PRL is located at the upper left quadrant. The retinal sensitivity in this area is unknown due to the PRL being slightly outside the range of the perimetry test. The optic nerve located on the right side of the visual field as well as blood vessels were used in identifying the PRL location in relation to the perimetry results (see figure 14).

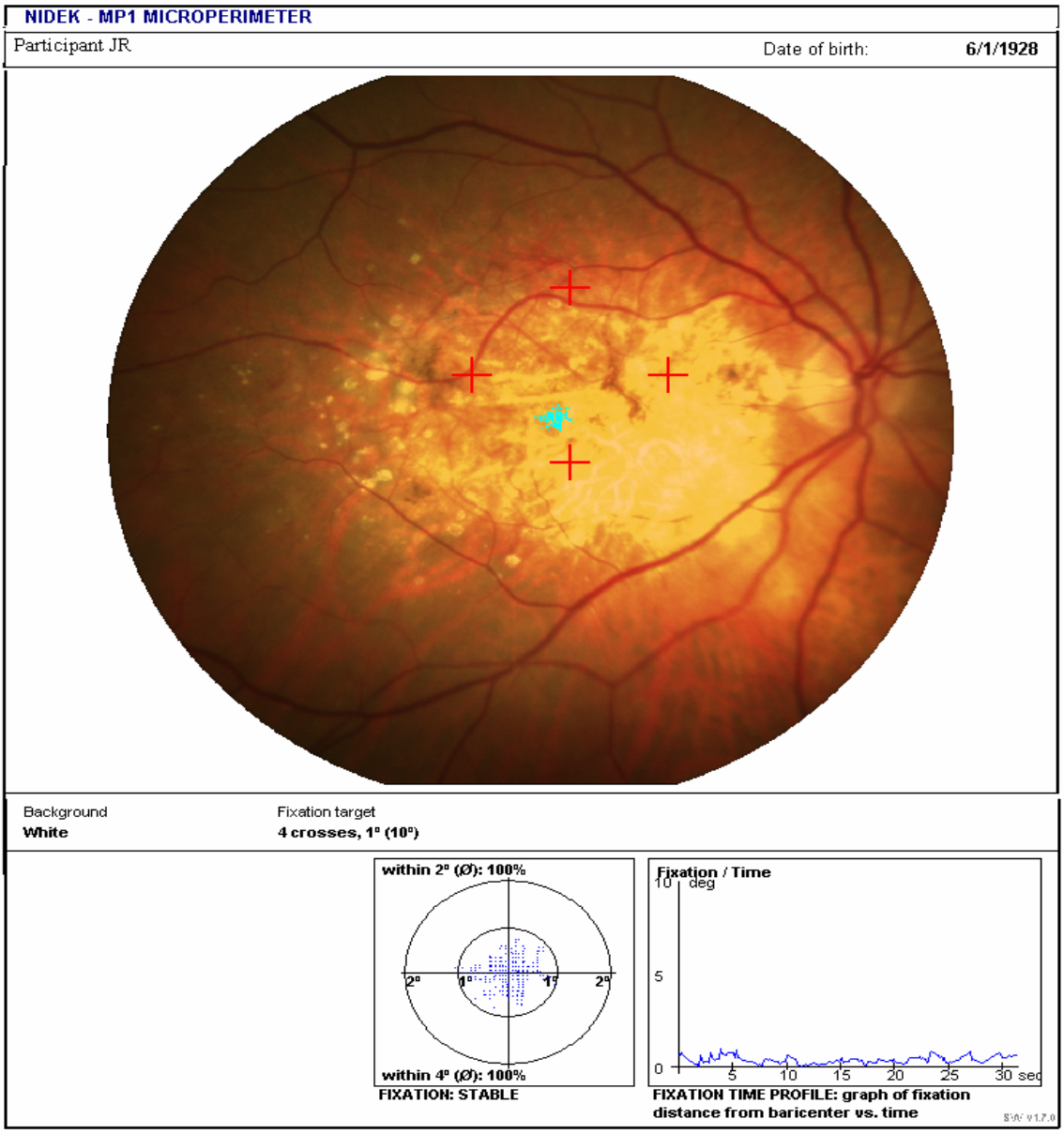

Figure 18: JR MP-1 Four cross fixation test

Using the optic nerve and blood vessels as reference positions in the figure above, the locations of participant JR's PRL and fovea were determined to be different. The fixation positions

in the scatter plot show participant JR's fixation to be within one degree eccentricity of the visual field.

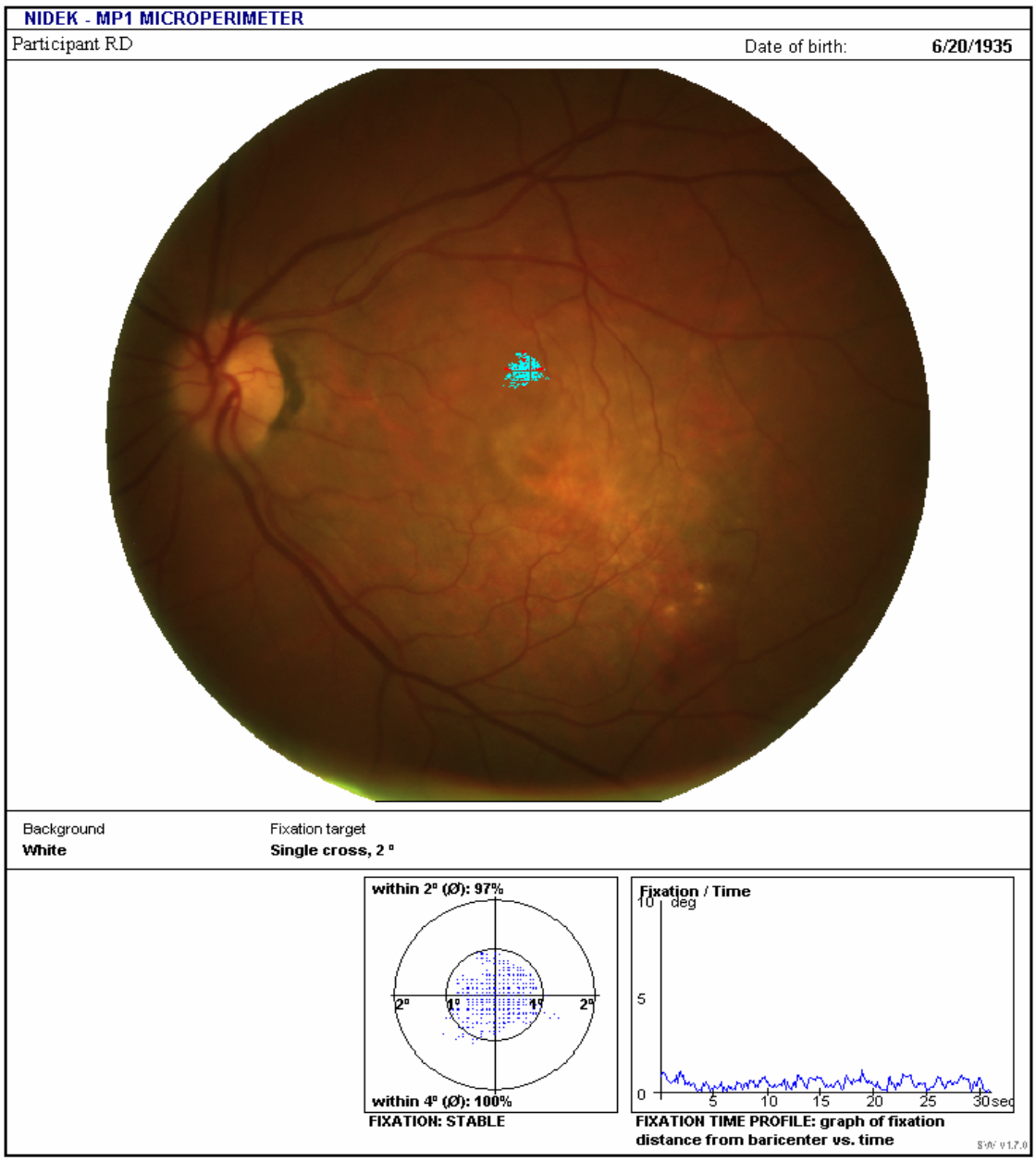

Figure 19: RD MP-1 single cross fixation test

In comparing figures 15 and 20, participant RD's PRL is at about 4 degrees above the fovea and has a retinal sensitivity at 8dB. The scatter plot and line graph in the figure above show participant RD fixates mostly within one degree eccentricity of the visual field.

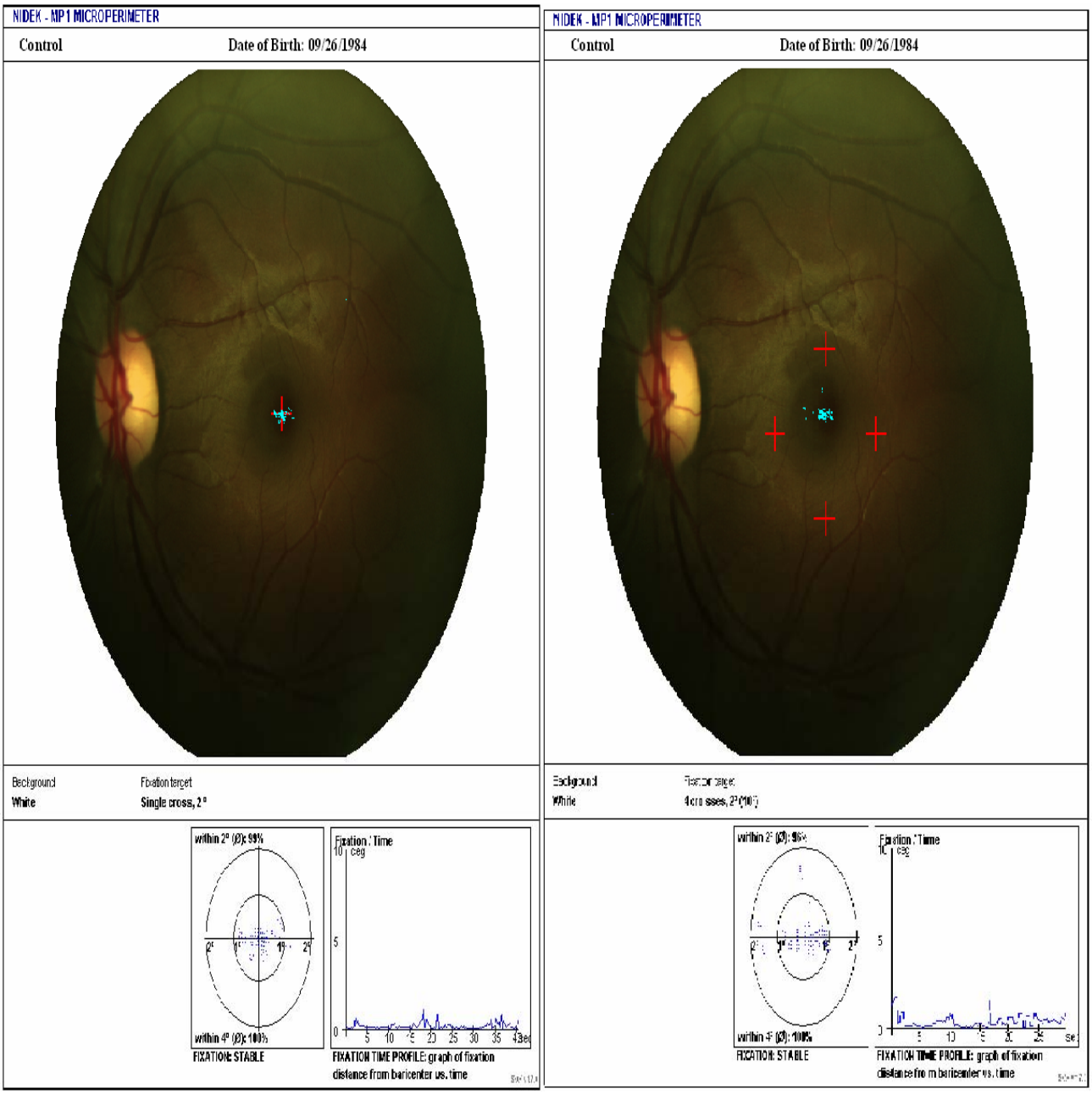

Figure 20: Control Single and Four cross fixation test (Left Eye)

Figure 20 shows the fixation pattern of the control participant's left eye for the single cross and four cross fixation test. The fixation positions are all within one degree eccentricity (except for a few drifts in the four cross fixation test) and mostly confined along the horizontal axis of the cross.

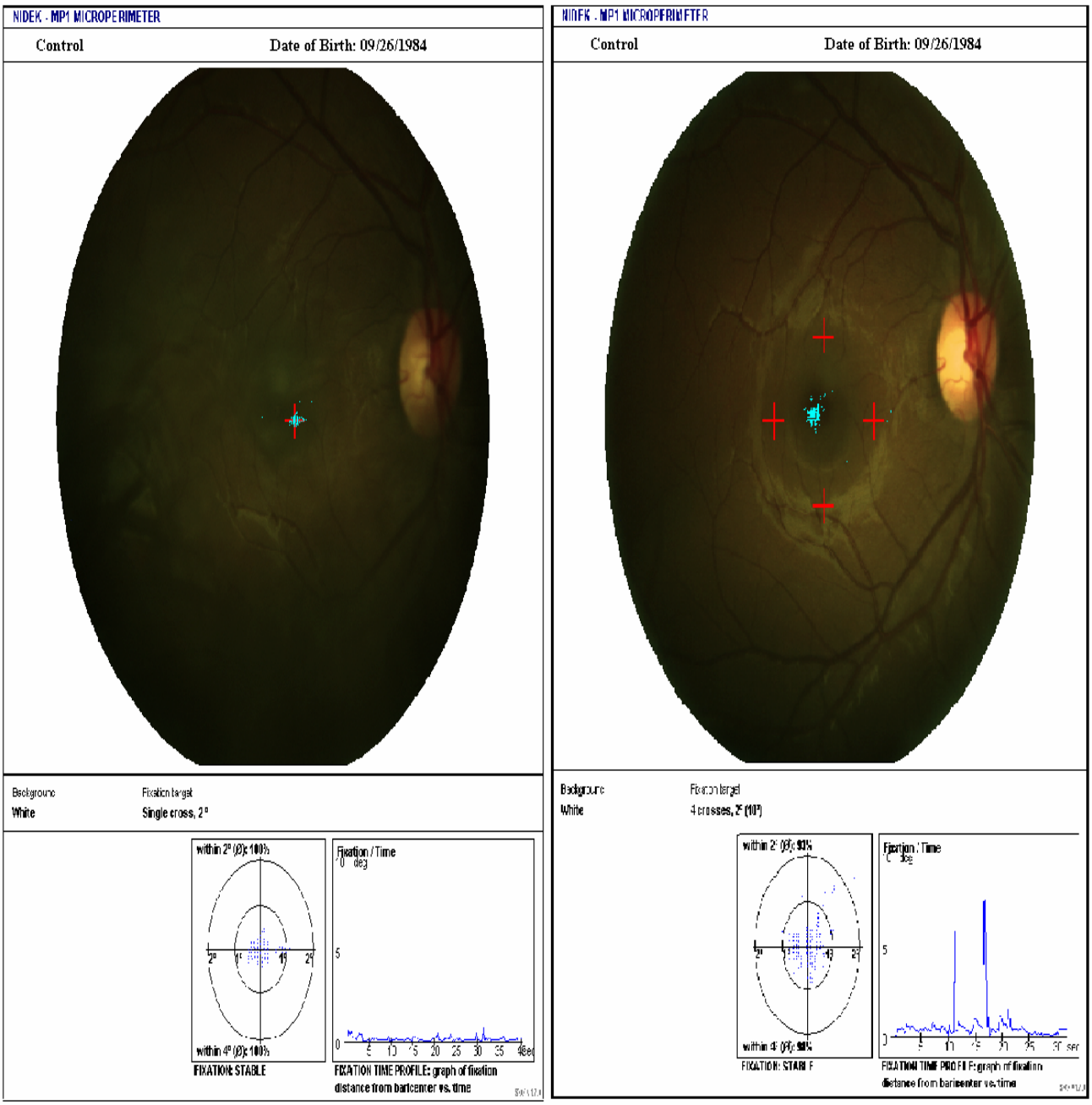

Figure 21: Control Single and Four cross fixation test (Right eye)

The fixation positions above are collected from the control participant's right eye. A few drifts during the four cross fixation test occurred but the control participant's fixation positions are mostly centered at the fovea in both fixation tests. The fixation positions are also mostly within one degree eccentricity in both fixation tests except for a few fixation positions in the four cross fixation test.

7.3 PEER: Optimal Parameters

The following results were obtained while investigating the optimal PEER parameters of TR and scanned brain volume. The variation of these two parameters led to changes in the measured signal to noise ratio (SNR) and thus influenced PEER's estimations. The PEER estimations analyzed were obtained from a training set made up of three concatenated calibration sets. The results are presented below in terms of standard error and standard deviation. The standard error represents each participant's deviation from the stimulus positions displayed while the standard deviation represents the variance of the point of gaze estimations at each TR and/or number of scanned slices.

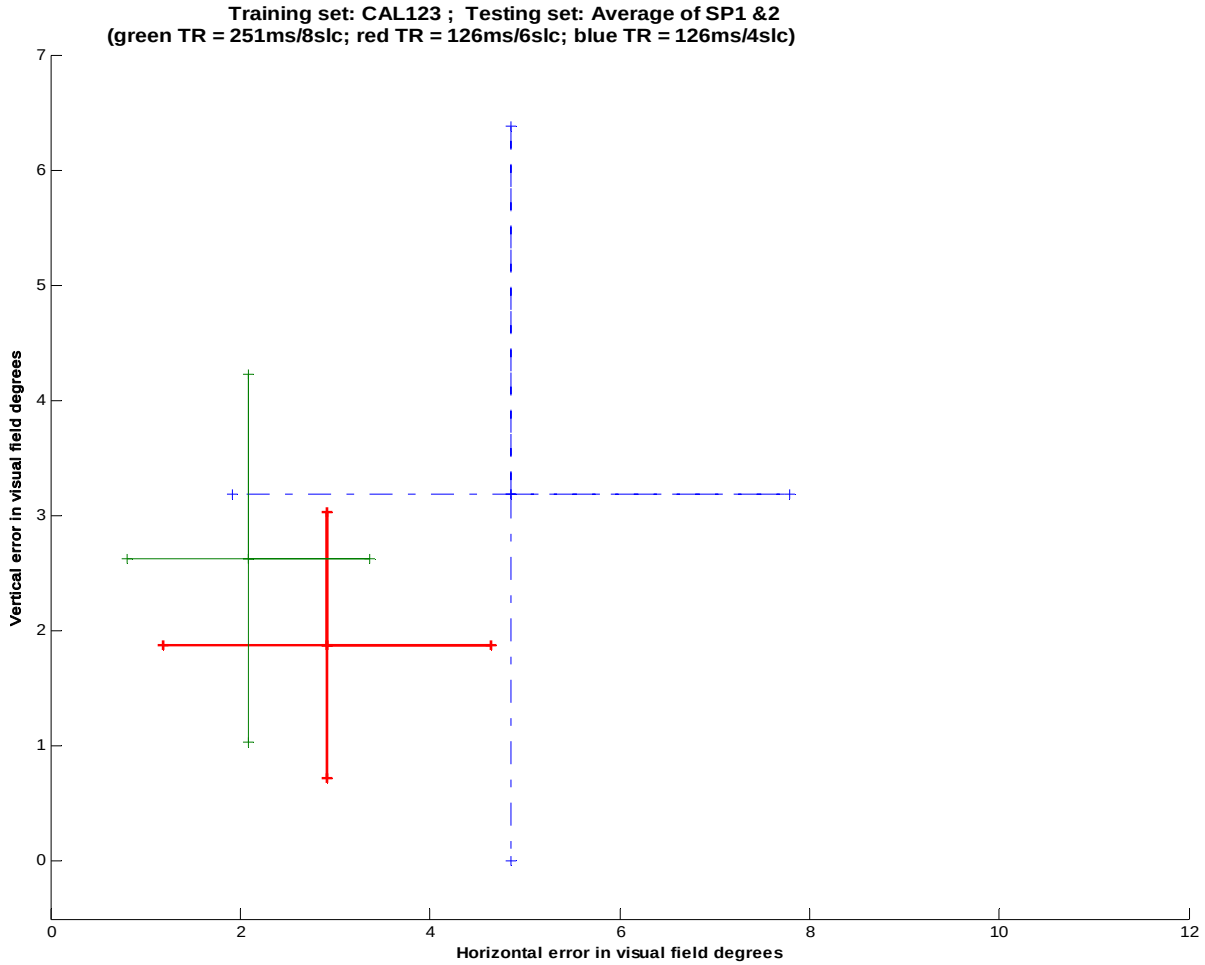

Figure 22: Average of smooth pursuit 1&2 (SP1&2)

In the figure above, the blue dashed line represents the condition: TR = 126ms/ 4 scanned slices through the eyes. It shows that the TR of 126ms (4slices) produces the poorest estimation of

the participant's fixation positions in both smooth pursuit tasks. This is seen through the high vertical and horizontal standard error and standard deviation results of this condition. This result is also supported by the Levene test (Table 3) which shows the TR of 126ms (4 slices) to be significantly different from the other two conditions.

Table 3: Variance and Levene's Test of Equality of Error Variances

Task	**TR=126ms / 4slc Variance (X,Y)**	**TR=189ms / 6slc Variance (X,Y)**	**TR=251ms / 8slc Variance (X,Y)**	**Levene's Test**
SP 1	(13.958, 3.254)	(3.201, 0.755)	(1.080, 1.679)	F (2, 3741) = 1137.66; $p < 0.05$
SP 2	(4.537, 2.358)	(2.772, 2.081)	(2.772, 2.081)	F (2, 3739) = 70.15; $p < 0.05$
SP avg.	(8.608, 10.176)	(2.983, 1.336)	(1.638, 2.538)	F (2,3741) = 767.30; $p < 0.05$

In choosing the optimal PEER parameters from the results above two criteria were considered. First, the TR had to produce a dense sample of eye movements and it had to be within or below the MD gaze duration of 250-350ms. Second the TR had to produce a reasonably low variability in its point of gaze estimations. A scanned brain volume of six slices and a TR of 189ms were chosen as the best fit to these criteria.

7.3 PEER: Participant results

The PEER estimations below were obtained from a model trained on six concatenated calibration sets. These estimations are presented as standard error and standard deviation for all eye movement tasks (i.e. random fixation and smooth pursuit) and for both the single cross and four cross fixation tests. Here, the standard error represents the participant's deviation from the presented stimulus position and the standard deviation his/her level of fixation instability during the task.

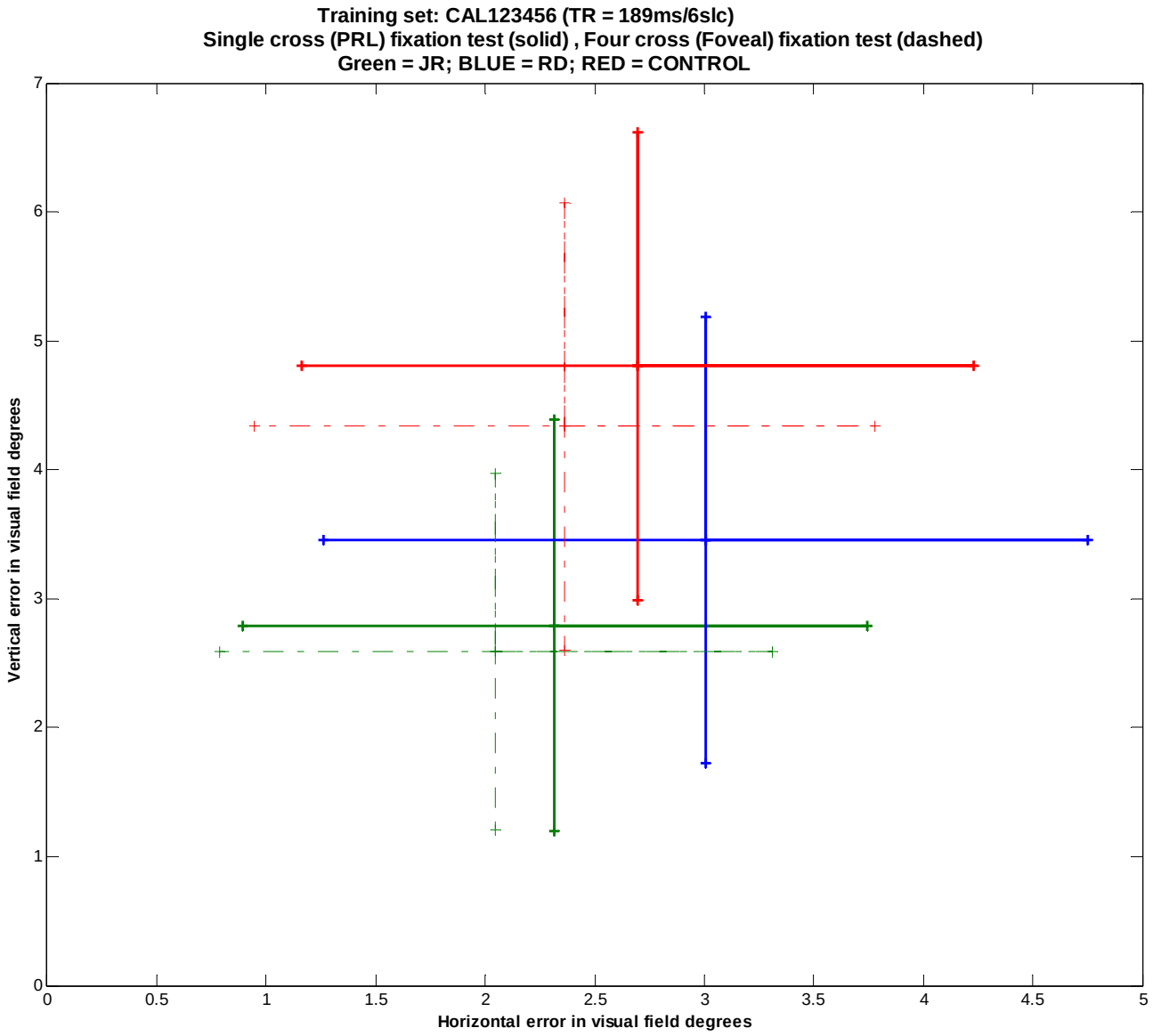

Figure 23: Single cross and Four cross fixation test

In the figure above, all single cross fixation test results are displayed as solid lines while the four cross fixation test results are displayed as dashed lines. In the single cross fixation test, the control participant (red solid line) shows the worst fixation accuracy overall while participant JR (green solid line) shows the best fixation accuracy with the lowest fixation error in both the vertical and horizontal axis. In the four cross fixation test the control participant also has the highest standard error in the vertical and horizontal axis and thus performed worse than participant JR.

All participants show similar standard deviation in both the single and four cross fixation tests. Participant JR and the control participant are shown to have better fixation stability at their fovea. Levene's test (see Table 4) demonstrates participant JR and the control participant have better fixation stability in the four cross fixation tests.

Table 4: Levene's test on PEER's Fixation test results

Participant	Single cross variance (X,Y)	Four cross Variance (X,Y)	Levene's Test
Control	(2.350, 3.305)	(2.008, 3.010)	$F(1,316) = 14.34$; $p < 0.05$
RD	(3.042, 3.000)	N/A	N/A
JR	(2.033, 2.541)	(1.588, 1.910)	$F(1,316) = 13.90$; $p < 0.05$

The units of the results in the table are in visual field degrees.

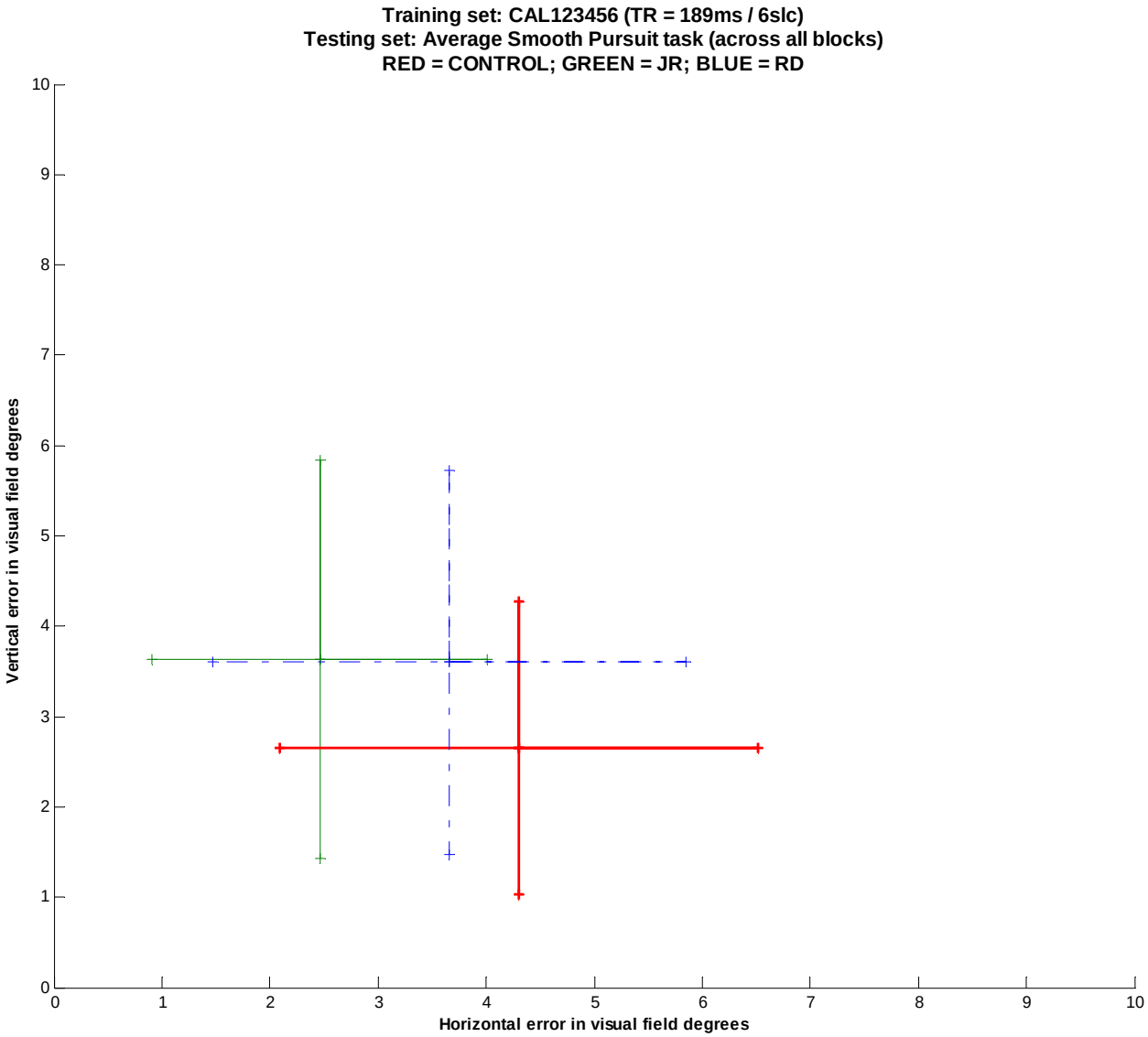

Figure 24: Smooth Pursuit (2nd PEER stage)

Figure 24 shows the average results of all the smooth pursuit task blocks in all participants. The figure suggests all participants possess similar fixation stability. In terms of fixation accuracy, the control participant deviates most in the horizontal direction and least in the vertical direction. In addition, the standard error results in the vertical axis are similar in both MD participants.

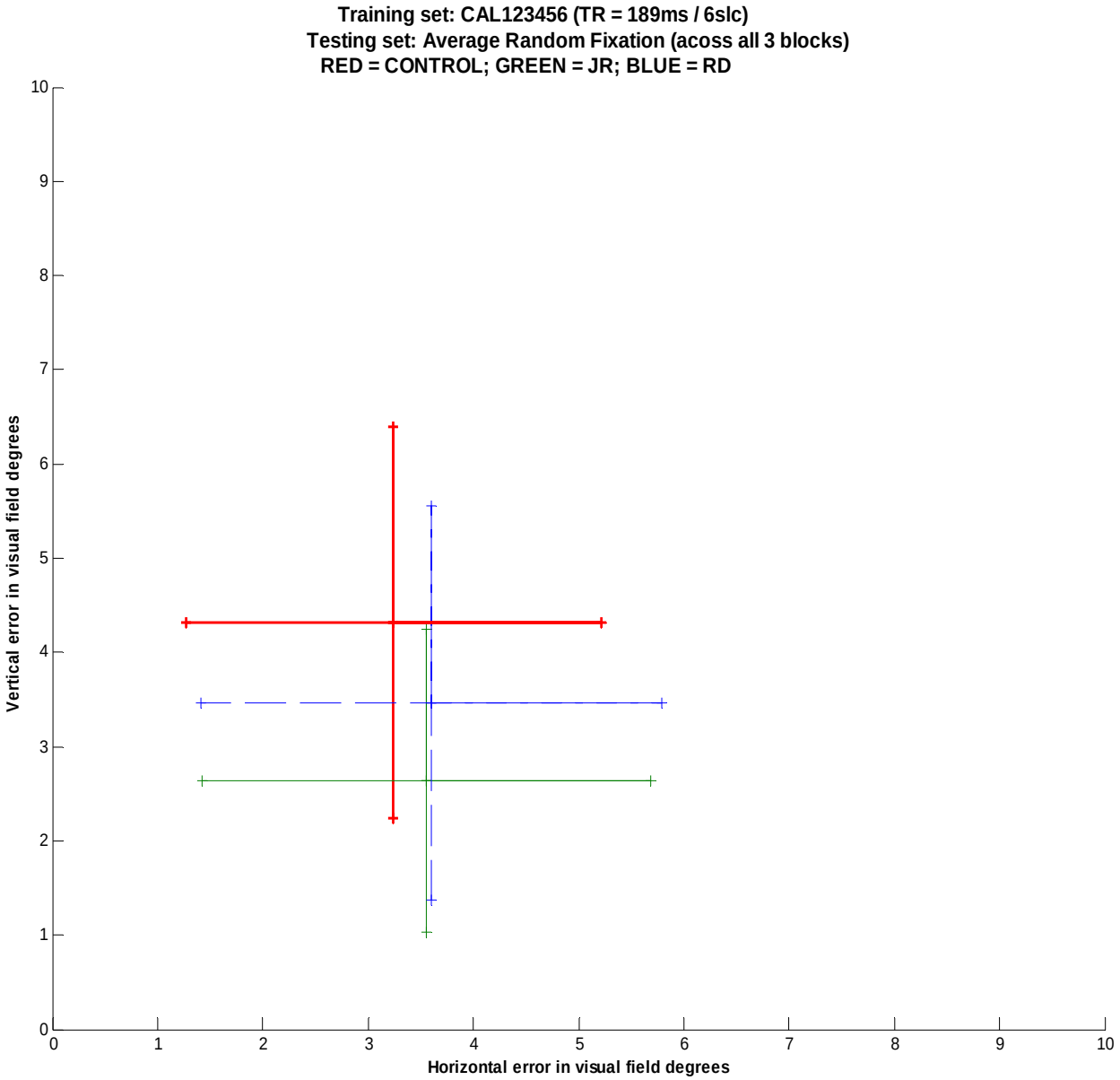

Figure 25: Random Fixation (2nd PEER stage)

Figure 25 suggests all participants to have similar fixation stability in both the vertical and horizontal direction (see table 5). Fixation accuracy, on the other hand, is different among the participants especially in the vertical direction. The control participant shows the worst fixation accuracy in this direction. In the horizontal direction, only a slight difference is seen between all participants. The control participant fixation accuracy is slightly better than that of the MD participants in this direction. Table 5 gives the variance for the vertical and horizontal axes, showing the fixation instability each participant exhibited during the two tasks.

Table 5: Variance in smooth pursuit and random fixation task

Participant	Smooth Pursuit variance (X,Y)	Random Fixation variance (X,Y)
Control	(4.902, 2.641)	(3.881, 4.318)
RD	(4.800, 4.541)	(4.805, 4.368)
JR	(2.394, 4.875)	(4.533, 2.586)

CHAPTER 8: DISCUSSION

8.1 MP-1 results

Participant JR's perimetry results show that the use of a dominant PRL is not dependent on the area of highest retinal sensitivity (see figures 14 and 17). In the single cross and four cross fixation tests, participant JR's fixation was classified as stable. Participant JR is thus able to reliably fixate using the fovea and still effectively use a PRL. Participant RD's fixation in the single cross fixation test was also classified as stable (figure 19). Thus, RD's dominant PRL was stable. The MD participants all had fixation positions within two degrees radius of the fovea and are therefore supported by the 1 - 9 degree range reported for MD patient fixation in Schuchard (2005). In the control participant, the perimetry and fixation results show normal functioning of the retina in both eyes. All fixation test results classify the control participant's eyes as stable (figures 20, 21).

In the four cross fixation test, the control participant's fixation was observed to be less stable than fixation in the single cross fixation test (figures 20, 21). Participant JR's fixation, on the other hand, was observed to be better during the four cross fixation test than in the single cross fixation test (see figures17, 18). The control participant's was worse fixation in the four cross fixation test, a result supported by Bellmann et al., (2004). However, Bellmann reported a no significant difference in MD patient fixation when using either peri-central or central fixation targets.

Altogether, the MP-1 shows that in an MD patient, fixation stability at the fovea can be just as functional as a normal sighted participant when conditions needed to aid fixation are met. Nevertheless, it should be noted that this outcome is reported in one MD participant and hence cannot be generalized to all MD patients.

8.2 PEER results

PEER's results were separated into the horizontal and vertical axes, providing more detail about each participant's fixation. Participant JR's fixation in both fixation tests and eye movement

tasks was classified as stable (figure 23-25, table 4 & 5). Participant JR's fixation in the four cross test was also determined to be significantly better than the single cross fixation test (table 4). Participant RD's fixation was classified as stable in the single cross test (figure 23, table 4). RD's fixation in the smooth pursuit and random fixation task were also stable (figure 24, 25 and table 5). The results from both eye movement and fixation tests thus identified participant RD's fixation as stable at the PRL. Fixation accuracy in both MD participants in the single cross fixation test and eye movement tasks was however relatively low – between 2 and 4 visual field degrees away from the fovea (figures 23-25). Thus, PEER shows both MD participants as able to steadily fixate but unable to accurately locate the stimulus target. The PEER estimated fixation stability in both MD participants is also supported by results reported in Schuchard (2005).

Fixation stability of the control participant was also classified as stable. The fixation stability in the control participant (in all tasks) was similar to that of the MD participants. The expected outcome for the control participant was greater fixation stability in comparison to the MD participants. However, PEER estimated a 0.5 degree difference in standard deviation (see table 4 and 5) between the control and MD participants; with MD patients mostly having more stable fixation. PEER also reports a significant difference between the four cross and single cross fixation test in the control participant (table 4); with the control participant having better fixation in the four cross test. This result is contrary to that reported by the MP-1 and in Bellmann, et al. (2004) and consequently raises questions as to PEER's accuracy and effectiveness in estimating point of gaze.

In terms of fixation accuracy, the control participant also showed slightly greater or similar standard error to the MD depending on the given direction (figures 23(single cross only)-25). Therefore, PEER determined the control participant's fixation characteristics to be similar and sometimes worse than the MD participants. This PEER outcome is again contrary to the expected result of the control having better fixation ability than the MD patients. However, as there was no

verification of each participant's exactness in task execution, PEER's validity cannot be entirely discredited.

8.3 Comparing MP-1 and PEER Fixation test results

Participant JR's fixation was classified as stable by both eye tracking systems. Both systems also showed JR's fixation during the four cross fixation test to be more stable than during the single cross test. Similar results were observed in participant RD. RD's fixation stability was classified as stable in both systems. In addition, the MP-1 showed most of RD's fixation positions as centered on the fixation cross while PEER showed RD's overall fixation to be about 2 degrees away from the center of the fixation cross in the single cross fixation test. In the control participant, the fixation stability results from both PEER and the MP-1 were equivalent. However, PEER's estimate of fixation accuracy for the control participant was poor in the single cross fixation test in comparison to the MP-1 results observed. This discrepancy in fixation accuracy suggests error in PEER's point of gaze estimates.

In addition, PEER shows the fixation stability in the four cross test to be better than the single cross test in the control participant while the MP-1 and Bellmann et al, (2004) show otherwise. The MP-1 also shows fixation precision in the single cross test to be better in the control than in the MD patients (figures17, 19-21). However, this result is not evident in PEER (figure 23). The discrepancies described above thus hinder the complete justification of PEER as an alternative fMRI eye tracking system for the neuroimaging of MD participants. Therefore, although there is a correspondence in fixation stability results across all participants in both eye tracking systems, PEER validity as an alternative eye tracking system can only be established if the source of this discrepancy is isolated and removed.

8.4 Limitations

Data from the MP-1 and the scanner were collected on the same day to avoid possible changes in retinal health in the MD participant. However, factors such as fatigue and inability to directly observe each participant's fixation while in the scanner prevents a definitive evaluation of each participant's accuracy in task execution. Thus, although the difference in fixation estimations made by PEER and the MP- 1 calls into question PEER validity as an alternative eye tracking approach, it is difficult to reach a conclusion on PEER's dependability. In addition, as a small number of MD patients with similar characteristics were tested in this study, the inclusion of more MD participants with different scotoma types will help provide a better estimate of PEER robustness and flexibility.

8.5 Future Work

The PEER data analysis in this study was done post hoc using MATLAB. However this analysis can also be done in real-time. The extension of PEER into real time application would provide significant impact to vision research. For example, real time fixation analysis can be applied to retinotopic studies in order to advance research into brain plasticity. Retinotopy is a neuroimaging paradigm used to describe the cortical organization of neuronal responses to visual stimuli. In MD patients with unstable fixation the results of a retinotopic study would prove unreliable. However with the application of real-time PEER, fixation positions that deviate from the target stimulus location can be removed in real time to enhance the correspondence between stimulated visual areas and the area of neuronal response.

Currently, the input vector (signal) fed into the SVM are the measured intensity voxel values of the brain. A summary of this signal, provided by extracting important components of these MR voxel intensity signals as relates to eye position could significantly improve the accuracy and reliability of PEER. Statistical methods such as principal component analysis are tools that can be

used to enhance the accuracy of PEER's estimations. Additional research is needed to explore the possibilities and limitations of PEER in relation to these techniques.

8.6 Conclusions

The results obtained identify PEER as a potential alternative to traditional eye tracking system in the MRI environment, particularly in reference to MD patients. The similarities seen in fixation stability classifications across both eye tracking systems highlights PEER's validity. However, more research is necessary to thoroughly assess PEER's reliability as an eye tracking system. For example, an eye tracker system that runs concurrently with PEER will help clear any uncertainty in regard to PEER's point of gaze estimations. In general, PEER holds promise as a valid alternative to the standard MRI eye tracker. Moreover, its possible extension into real time applications would make it a significant tool in neuroimaging and vision research.

References

Arroyo, J. G. (2006). "A 76-year-old man with macular degeneration." Journal of the American Medical Association, *295*(20), 2394-2406.

Aslin, R. N., McMurray, Bob (2004). "Automated corneal-reflection eye-tracking in infancy: Methodological developments and application to cognition." Infancy: 1-15.

Baker, C. I., Peli, E., Knouf, N., Kanwisher, N.G. (2005). "Reorganization of Visual Processing in Macular Degeneration." The Journal of Neuroscience 25(3): 614-618.

Bellmann, C., Feely, M., Crossland, M.D., Kabanarou, S.A., Rubin, G.S. (2004). "Fixation Stability Using Central and Pericentral Fixation Targets in Patients with Age-related Macular Degeneration." Ophthalmology 111: 2265-2270.

Bennett K.P. & Mangasarian. "Robust linear programming discrimination of two linearly inseperable sets." Optimization Methods and Software, 1:23-34, 1992.

Bird A. C., B. N. M., Bressler S. B., Chisholm I. H., Coscas G., Davis M. D., De Jong P. T. V. M., Klaver C. C. W., Klein B. E. K., Klein R., Mitchell P., Sarks J. P., Sarks S. H., Soubrane G., Taylor H. R., Vingerling J. R., (1995). "An international classification and grading system for age-related maculopathy and age-related macular degeneration." Survey of Ophthalmology 39(5): 367-374.

Boucard, C. C. (2006). Neuro-Imaging of Visual Field Defects. Laboratory of Experimental Ophthalmology. Netherlands, Uiversity Medical Center Groningen: 160.

Brewer, A. A., W. A. Press, et al. (2002). "Visual areas in macaque cortex measured using functional magnetic resonance imaging." Journal of Neuroscience 22(23): 10416-10426.

Burges, C. J. C. (1998). "A Tutorial on Support Vector MAchines for Pattern Recognition." Data Mining and Knowledge Discovery 2: 48.

Calford, M. B., Wang, C., Taglianetti, V., Waleszczyk, W. J., Burke, W., & Dreher, B. (2000). "Plasticity in adult cat visual cortex (area 17) following circumscribed monocular lesions of all retinal layers." Journal of Physiology-London, *524*(2), 587-602.

Cheung, S., Legge, G.E. (2005). "Functional and cortical adaptations to central vision loss." Vision Neuroscience 22(2): 187-201.

Crossland, M. D., L. E. Culham, et al. (2004). "Fixation stability and reading speed in patients with newly developed macular disease." Ophthalmic and Physiological Optics 24(4): 327-333.

Crossland, M. D. and G. S. Rubin (2002). "The use of an infrared eyetracker to measure fixation stability." Optometry and Vision Science 79(11): 735-739.

Darian-Smith, C., & Gilbert, C. D. (1995). "Topographic reorganization in the striate cortex of the adult cat and monkey is cortically mediated." Journal of Neuroscience, 15(3), 1631-1647.

Deruaz, A., Goldschmidt, Mira, Whatham, Andrew R, Mermoud, Christophe, Lorincz, Erika N, Schnider, Armin, Safran, Avinoam B (2006). "A technique to train new oculomotor behavior in patients with central macular scotomas during reading related tasks using scanning laser ophthalmoscopy: immediate functional benefits and gains retention." BMC Ophthalmology 6(35): 18.

Engbert, R. and K. Mergenthaler (2006). "Microsaccades are triggered by low retinal image slip." Proceedings of the National Academy of Sciences of the United States of America 103(18): 7192-7197.

Engel, S. A., G. H. Glover, et al. (1997). "Retinotopic organization in human visual cortex and the spatial precision of functional MRI." Cerebral Cortex 7(2): 181-192.

Evgeniou, T., M. Pontil, et al. (2000). "Statistical learning theory: A primer." International Journal of Computer Vision 38(1): 9-13.

Feret, A., S. Steinweg, et al. (2007). "Macular degeneration: Types causes, and possible interventions." Geriatric Nursing 28(6): 387-392.

Fletcher, D. C., R. A. Schuchard, et al. (1999). "Relative locations of macular scotomas near the PRL: Effect on low vision reading." Journal of Rehabilitation Research and Development 36(4): 356-364.

Gabriel, P., C. Kitchen, et al. (1988). "Effect of pupil size on kinetic visual field measurements." Clinical & Experimental Optometry 71(6): 184-187.

Gilbert, C. D. and T. N. Wiesel (1992). "Receptive-field dynamics in adult primary visual-cortex." Nature 356(6365): 150-152.

Gonzalez, E. G., Teichman J., Lillakas, L. Markowitz, S.N., Steinbach, M.J. (2006). "Fixation stability using radial gratings in patients with age-related macular degeneration." Can J Ophthalmology 14: 333-339.

Gonzalez, G., Teichman, J., Lillakas, L., Markowitz, S.N., Steinbach, M.J. (2006). "Fixation stability using radial grating in patients with age-related macular degeneration." Can J Ophthalmology 41: 333-339.

Goodrich, G. L. and E. B. Mehr (1986). "Eccentric viewing training and low vision aids - current practice and implications of peripheral retinal research." American Journal of Optometry and Physiological Optics 63(2): 119-126.

Hadjikhani, N., A. K. Liu, et al. (1998). "Retinotopy and color sensitivity in human visual cortical area V8." Nature Neuroscience 1(3): 235-241.

Heinen, S. J., & Skavenski, A. A. (1991). "Recovery of visual responses in foveal v1 neurons following bilateral foveal lesions in adult monkey." Experimental Brain Research, *83*(3), 670-674.

Horton, J. C., & Hocking, D. R. (1998). "Monocular core zones and binocular border strips in

primate striate cortex revealed by the contrasting effects of enucleation, eyelid suture, and retinal laser lesions on cytochrome oxidase activity." Journal of Neuroscience, 18(14), 5433-5455.

Joachims, T. (1998a). Text Categorization with Support Vector Machines: Learning with Many Relevant Features. European Conference on Machine Learning, Springer.

Joachims, T. (1999a). Making large-Sclae SVM Learning Practical, MIT Press.

Joachims, T. (1999c). Transductive Inference for Text Classification using Support Vector Machines. International Conference on MAchine Learning (ICML).

Joachims, T. (2002a). Learning to Classify Text Using Support Vector Machines.

Kaas, J. H., Krubitzer, L. A., Chino, Y. M., Langston, A. L., Polley, E. H., & Blair, N. (1990). "Reorganization of retinotopic cortical maps in adult mammals after lesions of the retina." *Science, 248*(4952), 229-231.

Kamitani, Y., Tong, Frank (2005). "Decoding the visual and subjective contents of the human brain." Nature Neuroscience 8(5): 679-685.

Kosnik, W., J. Fikre, et al. (1986). "Visual fixation stability in older adults." Investigative Ophthalmology & Visual Science 27(12): 1720-1725.

la Cour, M., Kiilgaard, Jens Folke, Nissen, Mogens Holst (2002). "Age-Related Macular Degeneration: Epidemiology and Optimal Treatment." Drugs Aging 19(2): 101-133.

LaConte, S., J. Anderson, et al. (2003). "The evaluation of preprocessing choices in single-subject BOLD fMRI using NPAIRS performance metrics." Neuroimage 18(1): 10-27.

LaConte, S., Glielmi, C., Herberlein, K., and Hu, x. Verfiying visual fixation to improve fMRI with predictive eye estimation regression (PEER). Inetrnational Society of Magnetic Resonance in Medicine.

LaConte, S., Peltier, S, Heberlein, K.A., Hu, X.P. Predictive Eye Estimation Regresion (PEER) for Simaltaneous Eye Tracking and fMRI. International Society of Magnetic Resonance in Medicine.

LaConte, S., Peltier, S, Hu, X. (2006). "Real-time fMRI using brain-state classification." Human Brain Mapping.

LaConte, S., Peltier, S.J., Hu, X.P. (2006) Real-time fMRI using brain state classification. Volume, DOI: 10.1002/hbm.20326

LaConte, S., S. Strother, et al. (2005). "Support vector machines for temporal classification of block design fMRI data." Neuroimage 26(2): 317-329.

Laconte, S., S. Strother, et al. (2003). "Predicting Motor Tasks in fMRI Data with Support Vector Machines." Proc. Intl. Soc. Mag. Reson. Med. 11: 494.

Land, M. F. and S. Furneaux (1997). "The knowledge base of the oculomotor system." Philosophical Transactions of the Royal Society of London Series B-Biological Sciences 352(1358): 1231-1239.

Lei, H. and R. A. Schuchard (1997). "Using two preferred retinal loci for different lighting conditions in patients with central scotomas." Investigative Ophthalmology & Visual Science 38(9): 1812-1818.

Martinez-Conde, S., S. L. Macknik, et al. (2006). "Microsaccades counteract visual fading during fixation." Neuron 49(2): 297-305.

Martinez-Ramon, M., V. Koltchinskii, et al. (2006). "fMRI pattern classification using neuroanatomically constrained boosting." Neuroimage 31(3): 1129-1141.

McFadzean, R. M., Hadley, D. M., & Condon, B. C. (2002). "The representation of the visual field in the occipital striate cortex." *Neuro-Ophthalmology, 27*(1-3), 55-78.

McMahon, T. T., M. Hansen, et al. (1991). "Fixation characteristics in macular disease - relationship between saccadic frequency, sequencing, and reading rate." Investigative Ophthalmology & Visual Science 32(3): 567-574.

Moller, F. (2005). "Long-Term Follow-up of Fixation Patterns in Eyes With Central Scotomas From Georgraphic Atrophy That Is Associated With Age-related Macular Degeneration." Am J Ophthalmology 140: 1085-1093.

Moller, F., M. L. Laursen, et al. (2006). "The contribution of microsaccades and drifts in the maintenance of binocular steady fixation." Graefes Archive for Clinical and Experimental Ophthalmology 244(4): 465-471.

Mori, F., S. Ishiko, et al. (2001). "Scotoma and fixation patterns using scanning laser ophthalmoscope microperimetry in patients with macular dystrophy." American Journal of Ophthalmology 132(6): 897-902.

Murakami, I., Komatsu, H., & Kinoshita, M. (1997). "Perceptual filling-in at the scotoma following a monocular retinal lesion in the monkey." Visual Neuroscience, 14(1), 89-101.

Pidcoe, P. E. and P. A. Wetzel (2006). "Oculomotor tracking strategy in normal subjects with and without simulated scotoma." Investigative Ophthalmology & Visual Science 47(1): 169-178.

Raasch, T. W. (2004). "What we don't know about eccentric viewing." British Journal of Ophthalmology 88(4): 443-443.

Riusala, A., S. Sarna, et al. (2005). "Visual acuity and structural findings in old age-related macular degeneration." Graefes Archive for Clinical and Experimental Ophthalmology 243(9): 947-950.

Rolfs, M. (2007). In-Between Fixation and Movement: On the Generation of Microsaccades and What They Convey About Saccade Preparation. Human Sciences, University of Potsdam. Doctor of Philosophy: 1-183.

Schuchard, R. (2005). "Preferred retinal loci and macular scotoca characteristics in patients with are-related macular degeneration." Journal of Ophthalmology 40: 303-312.

Schuchard, R. A., PhD, Naseer, Saad, MD, De Castro, Kristina, MD (1999). "Characteristics of AMD patients with low vision receiving visual rehabilitation." Journal of Rehabilitation Research and Development 36(4): 1-13.

Schuchard, R. A. and T. W. Raasch (1992). "Retinal locus for fixation - pericentral fixation targets." Clinical Vision Sciences 7(6): 511-520.

Schumacher, E. H., J. A. Jacko, et al (in press). "Reorganization of Visual Processing is Related to Eccentric Viewing in Patients with Macular Degeneration." Restorative Neurology and Neuroscience.

Slotnick, S. D. and S. Yantis (2003). "Efficient acquisition of human retinotopic maps." Human Brain Mapping 18(1): 22-29.

Smirnakis, S. M., A. A. Brewer, et al. (2005). "Lack of long-term cortical reorganization after macaque retinal lesions." Nature 435(7040): 300-307.

Steinman, R. M. (1965). "Effect of target size luminance and color on monocular fixation." Journal of the Optical Society of America 55(9): 1158-&.

Straw, A.D., Warrant, E.J., & O'Carroll, D. C. (2006) A 'bright zone' in male hoverfly (Eristalis tenax) eyes and associated faster motion detection and increased contrast sensitivity. Journal of Experimental Biology 2006 209(21): 4339-4354.

Sunness, J. S., Liu, T., Yantis, S. (2004). "Retinotopic Mapping of the Visual Cortex Using Functional Magnetic Resonance Imaging in a Patient with Central Scotomas from Atrophic Macular Degeneration." Ophthalmology 111: 1595-1598.

Timberlake, G. T., M. A. Mainster, et al. (1986). "Reading with a macular scotoma .1. retinal location of scotoma and fixation area." Investigative Ophthalmology & Visual Science 27(7): 1137-1147.

Vapnik, V. (1995). The Nature of Statistical Learning Theory, New York: Springer Verlag.

White, J. M. and H. E. Bedell (1990). "The oculomotor reference in humans with bilateral macular disease." Investigative Ophthalmology & Visual Science 31(6): 1149-1161.

Whittaker, S. G., J. Budd, et al. (1988). "Eccentric fixation with macular scotoma." Investigative Ophthalmology & Visual Science 29(2): 268-278.

Whittaker, S. G., R. W. Cummings, et al. (1991). "Saccade control without a fovea." Vision Research 31(12): 2209-2218.